MALARIA

Antimalarial pantothenamide metabolites target acetyl–coenzyme A biosynthesis in *Plasmodium falciparum*

Joost Schalkwijk[1]*†, Erik L. Allman[2]*, Patrick A. M. Jansen[1]*, Laura E. de Vries[3]*, Julie M. J. Verhoef[3], Suzanne Jackowski[4], Peter N. M. Botman[5], Christien A. Beuckens-Schortinghuis[5], Karin M. J. Koolen[6], Judith M. Bolscher[6], Martijn W. Vos[6], Karen Miller[4], Stacy A. Reeves[4], Helmi Pett[3], Graham Trevitt[7], Sergio Wittlin[8,9], Christian Scheurer[8,9], Sibylle Sax[8,9], Christoph Fischli[8,9], Iñigo Angulo-Barturen[10], Mariá Belén Jiménez-Diaz[10], Gabrielle Josling[2], Taco W. A. Kooij[3], Roger Bonnert[11], Brice Campo[11], Richard H. Blaauw[5], Floris P. J. T. Rutjes[12], Robert W. Sauerwein[3,6], Manuel Llinás[2,13], Pedro H. H. Hermkens[14‡], Koen J. Dechering[6†‡]

Malaria eradication is critically dependent on new therapeutics that target resistant *Plasmodium* parasites and block transmission of the disease. Here, we report that pantothenamide bioisosteres were active against blood-stage *Plasmodium falciparum* parasites and also blocked transmission of sexual stages to the mosquito vector. These compounds were resistant to degradation by serum pantetheinases, showed favorable pharmacokinetic properties, and cleared parasites in a humanized mouse model of *P. falciparum* infection. Metabolomics revealed that coenzyme A biosynthetic enzymes converted pantothenamides into coenzyme A analogs that interfered with parasite acetyl–coenzyme A anabolism. Resistant parasites generated in vitro showed mutations in acetyl–coenzyme A synthetase and acyl–coenzyme A synthetase 11. Introduction and reversion of these mutations in *P. falciparum* using CRISPR-Cas9 gene editing confirmed the roles of these enzymes in the sensitivity of the malaria parasites to pantothenamides. These pantothenamide compounds with a new mode of action may have potential as drugs against malaria parasites.

INTRODUCTION

Malaria is a major global infectious disease that causes about 420,000 deaths per year, predominantly among children and pregnant women in sub-Saharan Africa (*1*). It is a vector-borne disease, and transmission depends on the transfer of sexually differentiated gametocytes from human peripheral blood to a mosquito vector. The clinical disease in the human host is caused by cyclic asexual parasite replication in red blood cells. Eradication of malaria is impeded by the ever-present rise of resistance to current drugs, including artemisinin derivatives, which calls for the urgent development of new antimalarial drugs (*2*). Ideally, new antimalarial drugs should have a new mechanism of action, no cross-resistance with existing drugs, and demonstrate activity against asexual and sexual blood stages and liver stages to prevent transmission of the disease (*3*). In addition, simple chemistry and resulting low manufacturing costs are important requirements to ensure access to new medicines for patients in low-income countries where malaria is endemic.

Pantothenate (pantothenic acid, vitamin B5, see Fig. 1A) is a water-soluble vitamin that is essential for malaria parasite viability (*4*). Pantothenate is required for the biosynthesis of coenzyme A (CoA), a cofactor involved in many metabolic processes, and this pathway has been explored as a potential antimicrobial target as early as the 1940s (*5*). Pantothenate utilization and CoA biosynthesis in *Plasmodium falciparum* have been extensively documented before (*6*–*9*), and these observations indicated that uptake of pantothenate and its conversion to CoA could be a viable drug target (*10*). A variety of pantothenate analogs, including pantoyltaurine, substituted pantoyltaurylamides, sulfonamides, pantothenol, and pantothenones, have shown antimalarial activity in avian (*5*) and mouse (*7*) malaria models. Pantetheine analogs based on N1 (substituted)-pantothenamides were initially shown to exert antibacterial activity in vitro (*11*). In *Escherichia coli*, pantothenamides were reported to enter the CoA biosynthesis pathway after phosphorylation by pantothenate kinase (PANK) and form antimetabolites that block CoA and acyl carrier–dependent processes (*12*–*14*). Despite their potent antimicrobial action in vitro, pantothenamides have never been developed into clinically effective drugs. This is due to their intrinsic instability in body fluids because they are hydrolyzed by the ubiquitous pantetheinase enzymes of the vanin family (*15*–*17*). Previous work has shown that pantothenamides are active against *P. falciparum* and bacteria in vitro, provided that serum pantetheinase activity is inhibited by heat inactivation or addition of a small-molecule vanin inhibitor (*16*–*18*). Recent reports have shown that modification of the linker between the two amides, e.g., by alteration of the linker length (*19*) or introduction of an α-methyl group (*20*), will increase their stability in serum. Such a modification was recently shown to have antimalarial activity in vivo (*21*). Other structural modifications to improve stability were directed at the labile amide bond

[1]Department of Dermatology, Radboud Institute for Molecular Life Sciences, Radboud University Medical Center, Nijmegen, Netherlands. [2]Department of Biochemistry and Molecular Biology and Huck Center for Malaria Research, The Pennsylvania State University, University Park, PA 16802 USA. [3]Department of Medical Microbiology, Radboud Institute for Molecular Life Sciences, Radboud University Medical Center, Nijmegen, Netherlands. [4]St. Jude Children's Research Hospital, Memphis, TN 38105, USA. [5]Chiralix, Nijmegen, Netherlands. [6]TropIQ Health Sciences, Nijmegen, Netherlands. [7]XenoGesis Ltd., Nottingham, UK. [8]Swiss Tropical and Public Health Institute, Basel, Switzerland. [9]University of Basel, Basel, Switzerland. [10]The Art of Discovery, Derio, Spain. [11]Medicines for Malaria Venture, Geneva, Switzerland. [12]Radboud University, Nijmegen, Netherlands. [13]Department of Chemistry, The Pennsylvania State University, University Park, PA 16802 USA. [14]Hermkens Pharma Consultancy, Oss, Netherlands.
*These authors contributed equally to this work.
†Corresponding author. Email: joost.schalkwijk@radboudumc.nl (J.S.); k.dechering@tropiq.nl (K.J.D.)
‡These authors contributed equally to this work.

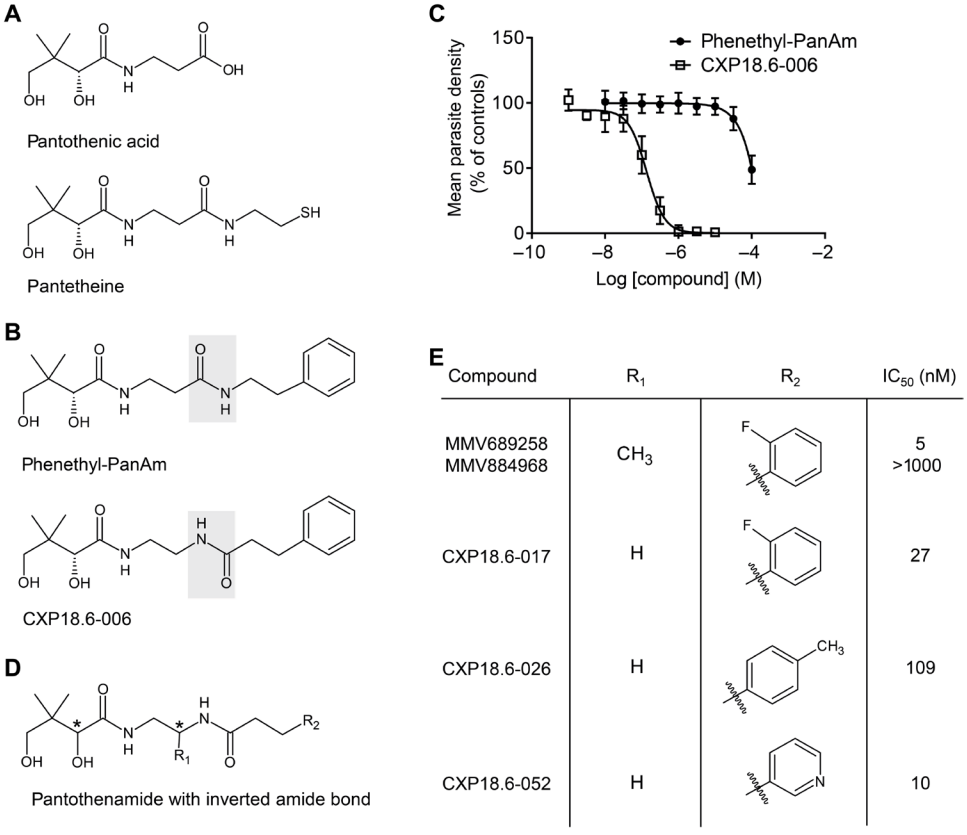

Fig. 1. Generation of stable pantothenamides. (**A**) Structures of pantothenic acid, the starting point of CoA biosynthesis, and pantetheine, a natural pantothenamide that is the substrate of vanins. (**B**) The structure of phenethyl-PanAm, the starting point for chemical optimization, and its stabilized analog CXP18.6-006. (**C**) The antimalarial activities of phenethyl-PanAm and CXP18.6-006 when tested against *P. falciparum* NF54 asexual blood-stage parasites in vitro. The figure shows mean parasite density relative to control. Error bars indicate SDs determined from four (phenethyl-PanAm) or three (CXP18.6-006) independent replicates. (**D**) The core structure of pantothenamides described in this paper. Chiral centers are indicated with an asterisk. (**E**) Structures of lead pantothenamide compounds and their IC_{50} values against asexual blood stages of *P. falciparum*. The active compound MMV689258 is in the 2′-*R*,2-*S* configuration, whereas the inactive compound MMV884968 is in the 2′-*S*,2-*R* configuration (table S1). R_1 and R_2 indicate positions in the core structure depicted in (D).

itself and introduced bioisosteric moieties in the classical pantothenamides (*22*, *23*). Studies on the mode of action of antimalarial pantothenamides have reported inhibition of *P. falciparum* PANK (*Pf*PANK) and formation of CoA antimetabolites (CoA-PanAm) as possible mechanisms (*21*, *24*, *25*). In rodent malaria parasites, the pantothenate transporter (PAT) and the downstream enzymes phosphopantothenoylcysteine synthetase (PPCS) and phosphopantothenoylcysteine decarboxylase (PPCDC) are essential for the development of the parasite in the mosquito midgut, suggesting that a drug interfering with this pathway may prevent disease transmission (*26*–*28*).

These findings motivated our search for new pantetheinase-resistant pantothenamide antimalarial drugs. Here, we present new pantothenamide analogs that are both stable, with the labile amide bond replaced by a pantetheinase-resistant bioisostere, and potent, with low nanomolar activity toward asexual and sexual blood stages of *P. falciparum*. Targeted metabolomics revealed that these new pantothenamides were metabolized by CoA biosynthetic enzymes and suppressed acetyl-CoA synthesis. We further demonstrated that these compounds were well tolerated and active in vivo using a humanized mouse model of *P. falciparum* infection. We also demonstrated that acetyl-CoA synthetase (*ACS*) and acyl-CoA synthetase 11 (*ACS11*) play crucial roles in the sensitivity of malaria parasites to pantothenamide compounds.

RESULTS

Development of stable pantothenamide bioisosteres

The starting point for chemical optimization of pantothenamides was *N*-phenethyl-pantothenamide (phenethyl-PanAm) (Fig. 1B), a previously described compound (*16*, *20*). This compound has potent antimalarial activity when protected from degradation by serum vanins through heat inactivation (*16*) or by the addition of a vanin inhibitor (*29*). A number of bioisosteric variations of the labile amide bond were designed, such as sulfone derivatives, five-membered heterocycles, and inverted amides, to improve stability in biological fluids (for examples, see table S1). For details about the synthesis and characterization of the compounds, see Supplementary Materials and Methods. Inversion of the amide yielded a pantothenamide bioisostere CXP18.6-006 (Fig. 1B) that was completely resistant to hydrolysis by serum-derived vanins as determined in vitro and in vivo (fig. S1). As a result, the compound was found to be several orders of magnitude more potent than the parent compound phenethyl-PanAm when tested for its ability to block replication of asexual blood stages of *P. falciparum* NF54 parasites in serum-containing medium (Fig. 1C). The structure-activity relationship in the series was further explored by a number of modifications of the core pantothenamide structure (Fig. 1D). Examples of these modifications and the resulting antimalarial activities are shown in table S1. The linker region between the two nitrogen atoms was scanned, and two carbons were found to provide the optimal chain length. Substitution at various positions of the ethyl linker showed that alkyl substitution with (*S*)-methyl at R_1 yielded a 10-fold increase in potency. This modification was previously described by others to improve the potency of phenethyl-PanAm (*20*). We tested a large number of modifications of the side chain (R_2 in Fig. 1D) based on the CXP18.6-006 backbone, as previously described (*22*). The results showed that substituted aryl, alkyl, and heteroaromatic side chains are tolerated at position R_2 (table S1). From this series of substitutions, four primary compounds emerged that provided potent antimalarial activity (Fig. 1E), with a 4-fluoro-substituted variant (MMV689258) as the most potent antimalarial compound. Investigation of the left-hand side of the molecule showed that the two hydroxyls and the two methyl groups were essential for activity (table S1). Previous work by others has shown that modification of the geminal methyl affects the antimicrobial

activity profile and blood stability of pantothenamides (*30*, *31*). With respect to stereochemistry, we observed that the *R* configuration of the secondary alcohol and the *S* configuration of the methyl at R_1 are preferred. MMV884968 (table S1), which is the 2′-*S*,2-*R* enantiomer of MMV689258, was found to be inactive (table S2).

Several pantothenamides inhibit both asexual replication and sexual parasite transmission

We investigated the effects of our four primary compounds at various stages of the parasite life cycle (fig. S2). All compounds inhibited replication of NF54 asexual blood-stage parasites with half maximal inhibitory concentration (IC_{50}) values <110 nM, with MMV689258 being the most potent compound at an IC_{50} of 5 nM (Fig. 2A and table S2). MMV689258 was active against a diverse panel of drug-resistant *P. falciparum* strains, suggesting a new mechanism of action (Fig. 2B and table S3). Despite highly potent activity against blood-stage parasites, only weak to moderate activity was seen against developing intrahepatocytic schizonts (Fig. 2C and table S2). On the basis of the observation that PAT, PANK, PPCS, and PPCDC in the pantothenate-CoA biosynthesis route are essential for parasite development in the mosquito midgut (*26*–*28*), we also investigated pantothenamide effects against the transmission stages of the parasite. To this end, mature gametocytes were incubated with compound for 24 hours and fed to *Anopheles stephensi* mosquitoes in a standard membrane-feeding assay (*32*). Eight days after feeding the infection, status of the mosquitoes was analyzed. The results showed that both CXP18.6-017 and MMV689258 prevented mosquito infection, with IC_{50} values that were comparable to their activity against asexual blood stages (Fig. 2D and table S2). This transmission-blocking activity relied on a gametocytocidal mode of action, as indicated by gametocyte viability assays that revealed IC_{50} values in line with the transmission blocking activity (Fig. 2E and table S2). Gametocytocidal activity varied in the series, and compound CXP18.6-052, for example, showed potent activity against asexual blood stages but not against gametocytes (table S2). Likewise, MMV689260, the 2′-*R*,2-*R* enantiomer of MMV689258, killed asexual blood stages with an IC_{50} of 210 nM but was inactive against gametocytes (table S1).

Pantothenamides are converted to CoA-PanAm and block acetyl-CoA synthesis

For all pantothenamides tested, the activity against asexual blood-stage parasites could be outcompeted with an excess of pantothenate (fig. S3A). Competition with pantothenate was also seen against liver-stage parasites for MMV689258, the only compound with IC_{50} <1 μM against this stage (fig. S3B). Conversely, the gametocytocidal activity

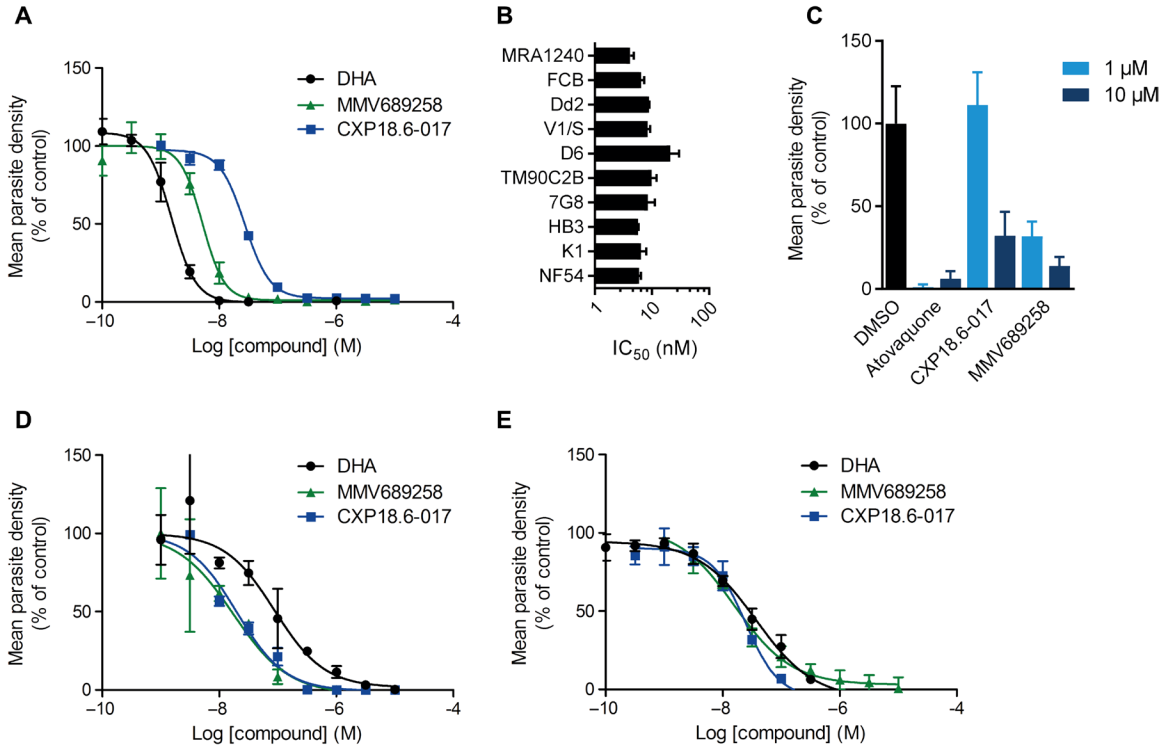

Fig. 2. In vitro antimalarial activities of pantothenamides. (**A**) The activity of pantothenamides against *P. falciparum* NF54 asexual blood-stage parasites in vitro. The figure shows mean parasite density relative to vehicle control. (**B**) The activity of MMV689258 against a panel of drug-resistant *P. falciparum* strains and, for comparison, against drug-sensitive NF54 parasites. (**C**) An analysis of the effects of MMV689258 on the development of *P. falciparum* NF54 parasites in human primary liver cells in vitro. The figure shows mean parasite density relative to vehicle control. (**D**) The transmission blocking activity of MMV689258. Mature *P. falciparum* stage V gametocytes from luminescent reporter strain NF54-HGL were exposed to compound for 24 hours before feeding to *A. stephensi* mosquitoes. Eight days after feeding, the infection status of the mosquitoes was assessed using luminescence analyses to count the number of oocysts. (**E**) The gametocytocidal activity of MMV689258 against *P. falciparum* NF54 gametocytes harvested at day 11 postinduction of gametocytogenesis in human red blood cells in vitro. (A), (B), (C), and (E) show average values and SDs from four to six replicates (A and E) or two to four replicates (B and C). (D) shows average values and SE of the mean from two independent mosquito feeding experiments with 15 to 24 mosquitoes per feeding experiment. DHA, dihydroartemisinin.

of pantothenamides was hardly sensitive to competition with pantothenate (fig. S3C), suggesting a stage-specific element in the mode of action, further evidenced by stage-specific killing activity for some compounds (tables S1 and S2). Measurements of free pantothenate concentrations in sera indicated average amounts of 0.33 μM in human serum (fig. S3D), which is below the baseline pantothenate concentration of 2.5 μM used in the parasitological assays. Serum pantothenate concentrations were found to be higher in mice and rats and averaged around 2 μM (fig. S3D).

Given the pantothenate-competitive activity in asexual blood-stage parasites, we addressed whether the compounds interfered with PANK, which was shown not only to be the rate-limiting step in the pantothenate-to-CoA conversion in other organisms (*33*), but it was also recently reported that mutations in the predicted *Pf*PANK1 conferred resistance to other pantothenate analogs (*25*). Phosphorylation of pantothenate was detected both in lysates of infected red blood cells and in uninfected red blood cells (fig. S4A). We generated a baculovirus-expressed recombinant form of *Pf*PANK1 (fig. S5A), but unfortunately, this protein was catalytically inactive in vitro. However, an antiserum generated against this protein (fig. S5B) successfully removed nearly all PANK activity from *P. falciparum* lysates (fig. S4, B and C), indicating that *Pf*PANK1 is likely to be the source of PANK activity in malaria parasites. Subsequent in vitro assays revealed that the pantothenamides competed with pantothenate phosphorylation by human and parasite PANK, albeit with relatively poor affinities, and the resulting IC_{50} values did not align with the in vitro antimalarial activities (fig. S4D and table S2). This suggested that parasite PANK activity was not the primary target for these compounds and led us to seek their mode of action.

Using an established high-performance liquid chromatography–mass spectrometry (HPLC-MS)–based metabolomics methodology for predicting the mode of action of antimalarial compounds (*34*), we tested the response to pantothenamides in purified trophozoite-stage parasites. In vivo modifications of pantothenamides by CoA biosynthetic enzymes have previously been reported in bacteria (*12*, *13*, *24*) and *Plasmodium* parasites (*24*). Therefore, we predicted and examined possible chemical derivatives on the basis of the structural and chemical features of the pantothenamides (table S4), as well as the endogenous metabolites involved in cellular CoA production (Fig. 3A). HPLC-based metabolomics confirmed that all of the tested antimalarial pantothenamides were ultimately converted to CoA-PanAm in red blood cells containing trophozoite stage parasites (Fig. 3B and fig. S6A). Similarly, and in line with the gametocytocidal activity of the compounds, CoA-PanAm was also detected in gametocytes (fig. S6B). The presence of an aryl group (R_2, Fig. 1D) in CoA-PanAm instead of a thiol, as observed in CoA, precludes further acetylation of CoA-PanAm and generation of the acetyl-CoA analog of the compound.

Targeted analyses of endogenous metabolites in the CoA pathway indicated that acetyl-CoA in asexual blood-stage infected erythrocytes was lower in the presence of the pantothenamides (Fig. 3C). Two of the compounds, CXP18.6-017 and CXP18.6-026, also resulted in large decreases of 4′-phosphopantothenate (Fig. 3C), a depletion that likely resulted from competition with endogenous pantothenate, because these compounds were tested at 10× the asexual IC_{50}, which approached the *Pf*PANK IC_{50} value (table S2). The detection of the phosphorylated form of the pantothenamides (4′-P-PanAm) confirmed that they were a substrate for *Pf*PANK, as previously reported by others (*24*) and competed with pantothenate when binding to the catalytic site. In gametocytes, incubation with 1 μM MMV689258 for 2.5 hours resulted in similar changes in endogenous metabolites in the CoA biosynthesis pathway (fig. S6C). Within a time frame of 2.5 hours, no additional changes were identified in asexual parasite metabolism (Fig. 3C and fig. S6D), further demonstrating CoA pathway specificity.

To delineate red blood cell and parasite-mediated metabolism, saponin lysis was used to isolate trophozoite-stage parasites from infected human red blood cells (fig. S7A). Incubation of free parasites with 1 μM MMV689258 for 3 hours in pantothenate-free media led to accumulation of CoA-MMV689258 (fig. S7B). In control experiments with uninfected red blood cells, CoA-MMV689258 was also observed, and the amounts were comparable to those observed in parasites (fig. S7B). This was quite unexpected, given that a parallel experiment performed with isotopically labeled pantothenate demonstrated that red blood cells do not readily metabolize pantothenate. De novo generated labeled acetyl-CoA concentrations in red blood cells were negligible, as values were at or below background spectral noise (fig. S7B). Although human red blood cells appeared to lack the complete set of enzymes required for de novo CoA synthesis (*35*), they do contain human PANK2 and CoA synthase, which explains the generation of CoA-MMV689258 in human red blood cells (Fig. 3A and fig. S7B). Acetyl-CoA amounts were unchanged in MMV689258-treated red blood cells (fig. S7C), which is in line with the lack of de novo synthesis in these cells. In contrast, free parasites readily converted radiolabeled pantothenate into acetyl-CoA. Accordingly, acetyl-CoA in free parasites dropped 15-fold after treatment with MMV689258 (fig. S7C), indicating that the reduction in acetyl-CoA observed in infected erythrocytes was due to a reduction of parasitic rather than red blood cell acetyl-CoA.

The observation that uninfected human red blood cells converted the pantothenamide bioisosteres to CoA-PanAm prompted us to investigate the effect of preexisting CoA-PanAm on parasite infection. Human red blood cells were pulsed with compound for 3 hours, followed by thorough washing and a 24-hour chase to allow conversion of the parent compound to the CoA-PanAm. Subsequently, the cells were infected with synchronized parasites that were allowed to proliferate for 72 hours. In this protocol, washout of the reference compound dihydroartemisinin did not inhibit parasite growth in drug-exposed cells (fig. S8A). In contrast, a 3-hour exposure of red blood cells to chloroquine, which is known to accumulate in red blood cells (*36*), was sufficient to exert a reduction in parasite replication. Likewise, parasites replicated poorly in red blood cells exposed to a pulse of MMV689258 before infection, suggesting that red blood cell–derived CoA-PanAm contributed to the pantothenamide mode of action. Parallel metabolomics experiments indicated that after an exposure of red blood cells to MMV689258 for 3 hours followed by washout, the upstream products rapidly diminished, and the resulting CoA-MMV689258 persisted for at least 72 hours (fig. S8B). The effect of red blood cell–derived CoA-MMV689258 on parasite replication implied that it can enter the cell, as has been suggested for CoA from phenotypic rescue experiments with exogenous CoA (*37*).

Mutations in *ACS* and *ACS11* confer resistance to pantothenamides

To further elucidate the mechanisms determining sensitivity to this class of pantothenamides, resistant parasites were selected by increased exposure to CXP18.6-052. Whole genome sequencing of five clones from two independent flasks revealed mutations in the gene coding

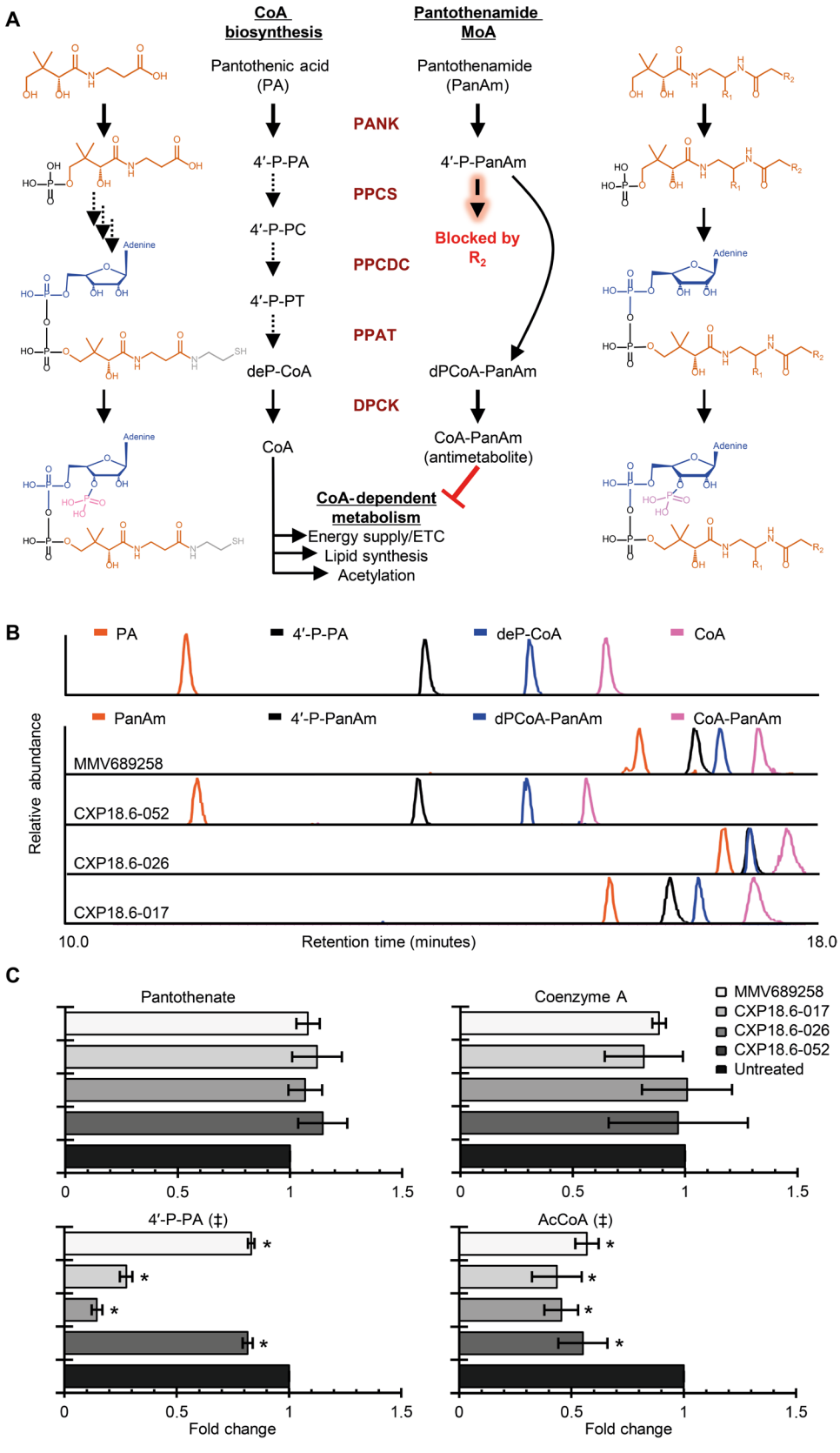

Fig. 3. CoA biosynthesis and pantothenamide metabolism in *P. falciparum* trophozoites. (**A**) Schematic for the endogenous pantothenate/CoA biosynthesis pathway (left) or pantothenamide metabolism (right). Structures are displayed for the metabolites of interest and colored to denote key functional residues. Enzyme abbreviations are displayed in red between the metabolic routes to denote the utilization of these enzymes in both pathways. PA, pantothenic acid; 4′-P-PA, 4′-phosphopantothenate; 4′-P-PC, 4′-phosphopantothenoyl-L-cysteine; 4′-P-PT, pantetheine-4′-phosphate; deP-CoA, dephospho-CoA; CoA, coenzyme A; PanAm, pantothenamide; 4′-P-PanAm, 4′-phosphopantothenamide analog; dPCoA-PanAm, dephosphoCoA pantothenamide analog; CoA-PanAm, pantothenamide CoA antimetabolite; ETC, electron transport chain; PANK, pantothenate kinase; PPCS, phosphopantothenoylcysteine synthetase; PPCDC, phosphopantothenoylcysteine decarboxylase; PPAT, phosphopantetheine adenylyltransferase; and DPCK, dephospho-CoA kinase. (**B**) Representative extracted ion chromatograms for pantothenate and pantothenamide metabolism. The top panel displays peaks for endogenous compounds run as pure standards (1 μM); antimetabolite peaks are from cellular extracts. The *x* axis denotes the retention time of the detected metabolite [colors match schematic in (A)], and the *y* axis denotes the relative abundance (100% per respective extracted ion chromatogram). All peaks identified were unique to the drug treatment (extracted ion chromatograms from untreated infected human red blood cell extracts not shown for clarity). (**C**) Endogenous metabolic alterations in trophozoite stage parasites treated with lead pantothenamide compounds at 10× IC_{50} for 2.5 hours. The *y* axis denotes the pantothenamide tested, and the *x* axis is the average peak area fold change (±SE) relative to a paired untreated control. Each sample was collected in technical triplicate for $n = 3$ biological replicates. ‡ denotes statistical significance at $P < 0.01$ by one-way ANOVA between all groups; * denotes $P < 0.01$ using Fisher's least significant difference post hoc method versus untreated control.

A

Gene	ID	Mutation	AA change	Flask/clone
PF3D7_0627800	Acetyl-CoA synthetase	ACA→GCA	T627→A	All
PF3D7_1238800	Acyl-CoA synthetase 11	AAA→AAC	K462→N	Flask 50/clones D3,D5,D12
PF3D7_1238800	Acyl-CoA synthetase 11	GAA→AAA	E660 →K	Flask 49/clones C5,C11

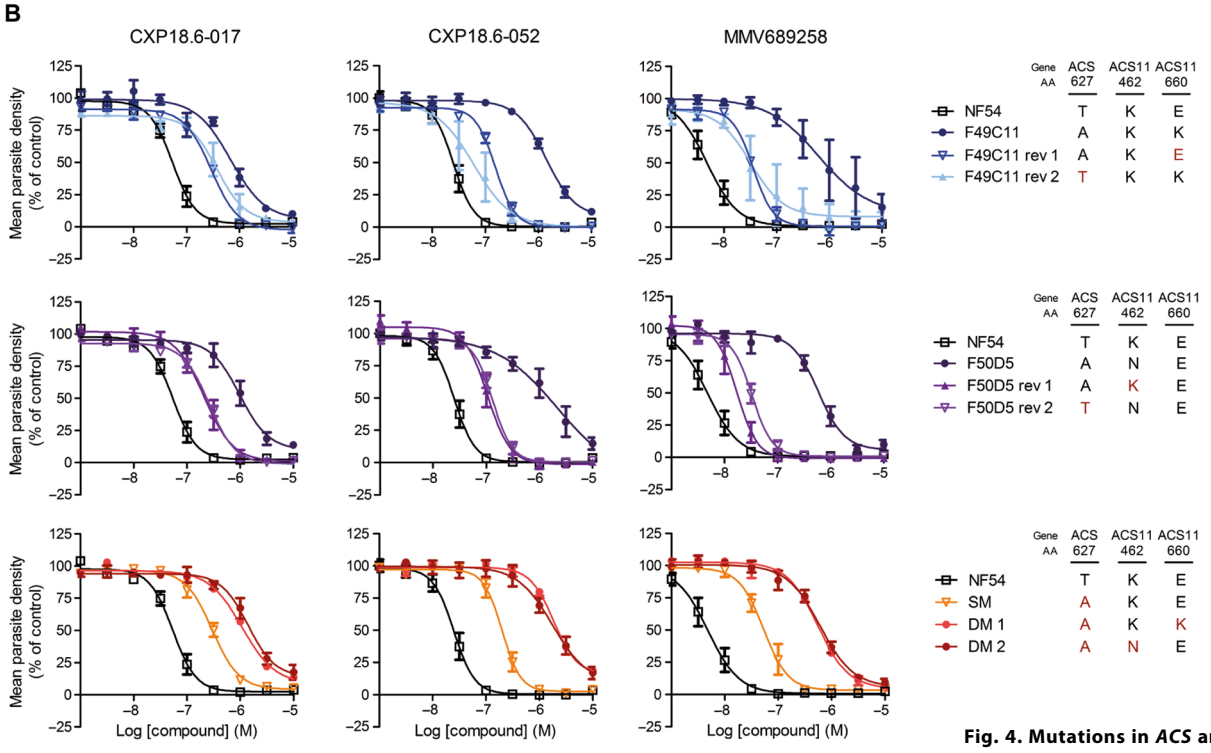

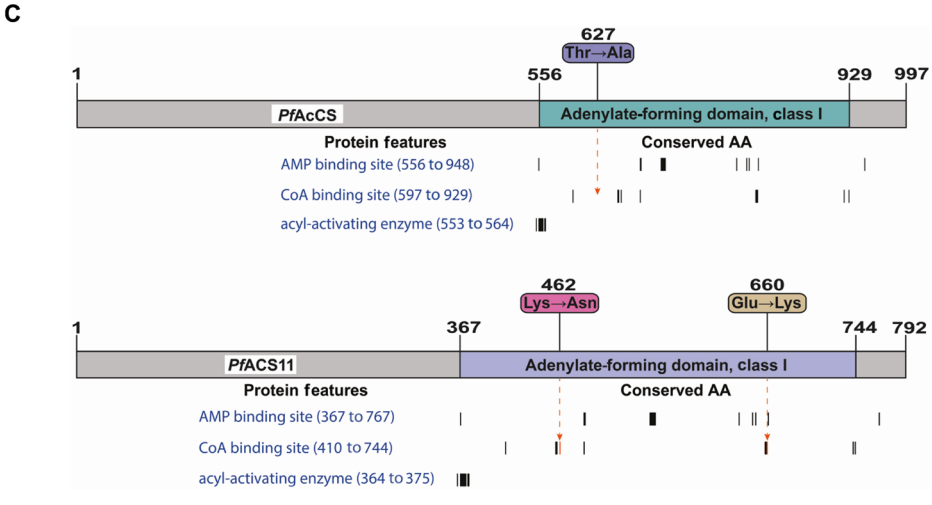

Fig. 4. Mutations in *ACS* and *ACS11* lead to pantothenamide-resistant parasites. (**A**) Listed in the table are mutations found in pantothenamide-resistant parasite lines that result in protein coding amino acid changes. Resistance against CXP18.6-052 was induced in NF54 parasites in two independent experiments. The mutations were identified from whole-genome sequences by comparison to the 3D7 reference genome and wild-type NF54 parental line. Multiple clones from each independently derived parasite line were sequenced. (**B**) Drug sensitivity assays for *P. falciparum* NF54 drug-induced resistant parasites (F49C11 and F50D5) and genetically engineered parasites. *ACS* and *ACS11* point mutations were either introduced in NF54 parasites or reverted in drug-induced resistant parasites using the CRISPR-Cas9 system. The graphs show average values for mean parasite density relative to controls for asexual blood-stage replication assays. Error bars indicate SEM determined from three independent replicates, with two to three technical replicates per experiment. The data were analyzed using nonlinear regression on GraphPad Prism. The amino acid changes in the different parasite lines are indicated in the key. Square, no mutation; triangle, single mutation; and circle, two mutations. rev, revertant; SM, single mutant; and DM, double mutant. (**C**) Schematic of protein domains and amino acid mutations. National Center for Biotechnology Information protein sequences were used to map protein domains annotated by the Conserved Domain Database. Black vertical bars denote conserved amino acids within a protein feature. Arrows demonstrate the mutation position within the protein feature; mutations that occurred in conserved amino acids are denoted in red.

for the fatty acid anabolism protein *ACS11* (PF3D7_1238800) for all clones. For two clones, the mutation resulted in an E660K amino acid change, whereas three clones contained a K462N substitution (Fig. 4A). Both mutations affected amino acid residues that are highly conserved across the CoA binding sites within the expanded 13-member *Plasmodium ACS* gene family (Fig. 4C)

(*38*). In addition to the *ACS11* mutation, all clones showed a common mutation in *ACS* (PF3D7_0627800), resulting in a T627A amino acid change (Fig. 4A). Whereas this residue is not conserved across species, it does fall within the CoA binding pocket (Fig. 4C). Last, all clones contained a common mutation in a single *var* gene (PF3D7_0900100), which encodes a highly polymorphic erythrocyte adhesion protein that is unlikely to contribute to the drug-resistant phenotype (*39*). Resistant parasites were able to produce gametocytes that infected *A. stephensi* mosquitoes (fig. S9). Asexual growth competition assays indicated that the drug-selected mutants did not show a growth advantage over wild-type parasites (fig. S10). The lack of sensitivity in the polymerase chain reaction (PCR) of the mutant allele did not allow us to robustly analyze a growth disadvantage induced by the resistance mutations and this awaits further study.

CRISPR-Cas9 engineering was used to further investigate the causal role of the *ACS* and *ACS11* mutations (fig. S11), because the encoded proteins are major contributors to parasite CoA metabolism (*40*). In comparison to the drug-resistant parent lines containing both mutations, reversion of either the *ACS* or *ACS11* allele back to wild type in these clones resulted in an intermediate drug resistance phenotype (Fig. 4B). Similarly, introduction of the *ACS*-T627A mutation in wild-type NF54 parasites resulted in an intermediate resistance phenotype (Fig. 4B). Engineering of this line to further introduce either the *ACS11*-K462N or *ACS11*-E660K substitution led to double mutants that phenocopied the drug-resistant clones selected through in vitro evolution. These data demonstrate that the combined mutations in *ACS* and *ACS11* together are sufficient to account for the observed pantothenamide resistance phenotype.

Metabolite profiling showed that the drug-resistant clone F50D5 containing the *ACS*-T627A and *ACS11* K462N substitution was fully able to convert MMV689258 into the CoA-PanAm form as expected, demonstrating that pantothenate metabolism was unaffected (fig. S12A). However, this clone showed a reduced sensitivity to inhibition of acetyl-CoA formation by MMV689258, in line with its drug-resistant replication phenotype (fig. S12B). Unlike wild-type parasites, the drug-resistant mutant showed a reduction in CoA at 1 μM MMV689258, a concentration that blocked replication of both wild-type and mutant parasites. This mutant-specific reduction in CoA may be due to a combined effect of the pantothenamide and the slow replication phenotype observed for the mutant.

MMV689258 suppresses parasitemia in a mouse model of human malaria infection

Pharmacokinetic experiments with MMV689258 revealed a moderate clearance of 50 ml min^{-1} kg^{-1} in mice and 23 ml min^{-1} kg^{-1} in rats with elimination half-lives of 1.8 and 3.6 hours, respectively (fig. S13 and table S5). The volume of distribution was 2.52 liters/kg in mice and 1.71 liters/kg in rats, and the compound was well absorbed upon oral dosing (bioavailability of 33.6% in mice and 63.4% in rats). Assessment of compound concentrations in urine and bile collected from rats showed that renal clearance contributed 26% to the total clearance, whereas biliary clearance was negligible (tables S6 and S7). On the basis of observed intrinsic clearance in rat hepatocytes of 2.0 μl/min per 10^6 cells (table S8), predicted in vivo hepatic clearance would amount to 14 ml min^{-1} kg^{-1}, which is in line with the nonrenal portion (17 ml min^{-1} kg^{-1}) of the total observed in vivo clearance, suggesting that the main route of elimination is through the liver.

To study the relationship between blood concentrations and parasite clearance, MMV689258 was tested in a humanized mouse model infected with *P. falciparum*. At single doses ranging from 25 to 200 mg/kg given 3 days after infection, parasitemia was reduced by 77 to 99.9% at day 7 compared to untreated control mice (Fig. 5A). Blood concentrations of MMV689258 in humanized mice showed a similar profile, as observed in initial mouse pharmacokinetic experiments (Fig. 5B). Analyses of dose-normalized data indicated that maximum concentration (C_{max}) and area under the curve ($AUC_{0–24}$) values were supraproportional with dose, suggesting possible saturation of clearance (fig. S14). With a measured fractional mouse plasma protein binding of 32.8% (table S8), total blood concentrations of 48.6 ng/ml would be required to achieve a free fraction above the in vitro determined IC_{99} (45 nM) of MMV689258. For all dosages, blood concentrations dropped below this level within 24 hours. Despite this rapid elimination, a single dose of 100 or 200 mg/kg continued to clear parasites 4 days after dosing. Parasite reduction upon prolonged exposure was further investigated in the humanized mouse model of *P. falciparum* infection by once daily dosing for 4 days. The results showed a dose-dependent reduction in parasitemia (Fig. 5C). The parasite reduction rates during the days of treatment showed a moderately fast profile, with rates in the 100 and 200 mg/kg dose groups that were similar to or slightly higher than that observed for chloroquine. In all dose groups, parasites recrudesced, with a delay of 5 days in the highest dose group.

In all animal experiments, drug administration was well tolerated, and no obvious acute adverse effects were noted. Moreover, we did not observe a detrimental effect on red blood cell counts in the humanized mouse experiments at any of the tested doses (fig. S15). In addition, MMV689258 and CXP18.6-017 did not inhibit hepatic CYP450 enzymes at concentrations of up to 20 μM, indicating a low risk for drug-drug interactions (table S2). In addition, metabolic profiling in primary human hepatocyte lines showed that pantothenamides readily entered liver cells, and similar to human red blood cells, convert only a small fraction of the total pool of compound to 4′-P-PanAm, dephosphoCoA-PanAm (dPCoA-PanAm), and CoA-PanAm (fig. S16A). In pantothenamide-exposed primary hepatocytes, acetyl-CoA showed a slight reduction of 20% with 1 μM MMV689258 (fig. S16B). However, we did not observe cytotoxic activity against HepG2, HC04 cell lines, or primary human hepatocytes in vitro (table S2). In addition, the amounts of endogenous metabolites in the pantothenate-CoA pathway were unaltered in red blood cells (fig. S7C). Whereas these initial experiments have demonstrated favorable toxicological profiles, selection of a pantothenamide clinical candidate will require further analyses of safety in in vitro and in vivo models.

DISCUSSION

Here, we describe new, stable pantothenamide bioisosteres that display potent activity against asexual blood stages of *P. falciparum*. A subset of compounds showed gametocytocidal activity and blocked transmission of blood-stage parasites to the mosquito vector. The most advanced compound, MMV689258, exerted antimalarial activity in a humanized mouse model of *P. falciparum* infection. Our findings support the advancement of stable pantothenamide bioisosteres for further evaluation of efficacy and safety in preclinical models. These compounds could be a useful addition to the antimalarial drug portfolio, because they (i) are straightforward to synthesize,

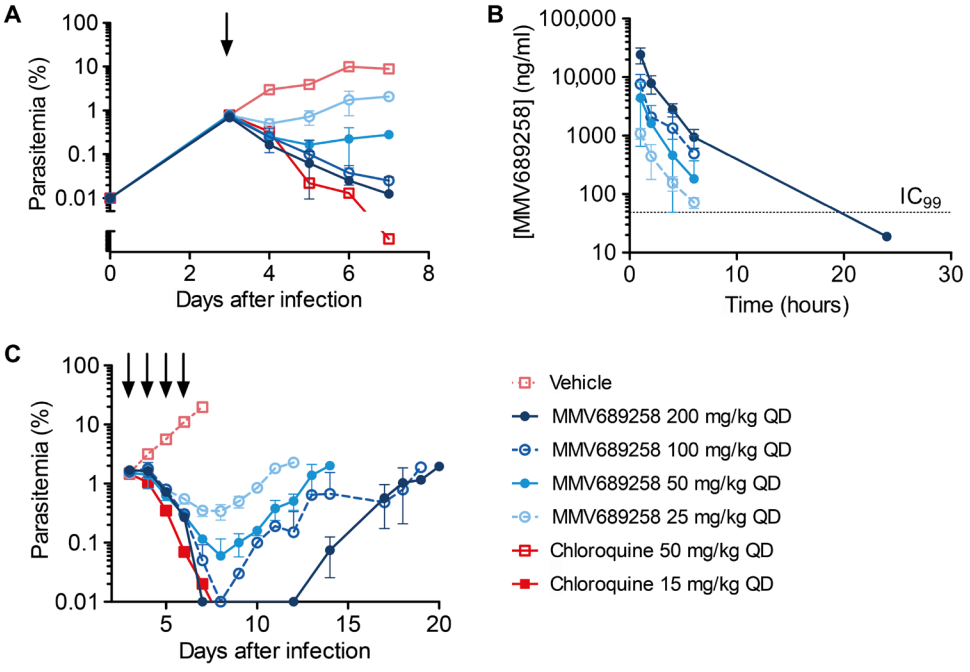

Fig. 5. In vivo efficacy and pharmacokinetics of MMV689258. Female NODscidIL2Rγ^{null} mice were engrafted with human red blood cells and infected with *P. falciparum* at day 0 at 1% and 2% parasitemia for the experiments depicted in (A) and (C), respectively. At day 3 after infection, mice were dosed with the compounds by oral gavage at doses indicated once daily (QD). (**A**) Parasitemia after a single dose of each compound (black arrow). (**B**) Blood concentrations of MMV689258 as a function of time after the first administration of compound at the doses indicated in the key. (**C**) Parasitemia after daily dosing with each compound on four consecutive days (black arrows). The graphs show average values and standard deviations from two mice per drug/dose combination.

(ii) can be manufactured at low cost, (iii) are transmission-blocking, and (iv) target a biochemical pathway that is not covered by currently marketed drugs.

Previous studies have demonstrated that antibiotics and antimalarial drugs based on the pantothenate/pantetheine scaffold are labile in biological fluids due to hydrolysis of the amide bond by serum vanins (*16*, *17*). Our data reveal that inversion of the amide bond afforded a considerable increase of stability while preserving the biological activity. Antimalarial activity was further improved by modification of the carbon linker and the aromatic ring of the side chain as reported in previous studies (*19*, *20*, *22*). Metabolomic analyses indicated that the pantothenamides use the CoA biosynthetic enzymes of both parasites and host red blood cells and are ultimately converted into CoA-PanAm. Because the pantothenamides lack the pantothenate carboxyl group, they bypass PPCS and PPCDC and are converted to the CoA-PanAm by PPAT and dephospho-CoA kinase (DPCK) upon phosphorylation by PANK. Consistent with this mechanism, our medicinal chemistry efforts revealed a narrow pharmacophore. All substitutions of functional groups that are essential for processing by PANK, PPAT, and DPCK, including the two alcohols and the dimethyl motif, led to a loss of antimalarial activity. The mechanism described here is consistent with the previously observed formation of a putative CoA-PanAm in infected red blood cells (*25*).

The in vivo efficacy studies presented here showed that after a brief exposure to MMV689258, parasitemia continued to decrease for a number of days before growth resumed. This may be the result of fast initial killing of the parasites, followed by a relatively slow elimination from the circulation. However, repeated dosing resulted in a greater total reduction of parasite numbers compared to single dosing. This suggests that parasite killing is not instantaneous, but that the reduction in parasitemia is rather driven by the time of exposure above a minimum parasiticidal concentration and the parasite killing rate, as has been demonstrated for other antimalarial compounds (*41*). The continued elimination of parasites after the point where MMV689258 plasma concentrations were undetectable may be explained by a postantibiotic effect, as observed for a number of antibacterial drugs (*42*). The nature of such effects is not well understood. For the pantothenamides described here, it may originate from accumulation of CoA analogs or their precursors, as observed in infected erythrocytes, parasites, and noninfected erythrocytes.

The observed recrudescence in a *P. falciparum*–infected humanized severe combined immunodeficiency (SCID) mouse model is in line with the short half-life of MMV689258 in mice, which precludes complete eradication of the parasites. In addition, the infected humanized mouse model may underestimate the efficacy of the compound because it is diluted by the daily supplementation of red blood cells and is competed by the high endogenous pantothenate concentrations in mice (sevenfold higher than in humans). Assuming that 70% of total clearance in humans would be contributed by the liver, as observed in rats, preliminary assessment of the in vitro clearance in human liver cells and allometric scaling of the rodent pharmacokinetics data suggest that the half-life in humans may be around 12 hours, which is ~7-fold longer than the half-life observed in mice. This suggests the possibility that, in humans, single dosing of MMV689258 may be able to maintain minimal parasiticidal concentrations for up to several days.

The data presented here demonstrate that modification of the pantothenamides by CoA biosynthetic enzymes produced antimetabolites that may interfere with downstream CoA-dependent processes. The observed decrease of acetyl-CoA in drug-exposed parasites is consistent with such a mechanism. Furthermore, selection and sequencing of drug-resistant parasite lines revealed mutations in two genes that encode the CoA-binding enzymes *ACS* and *ACS11*, which were confirmed upon genetic engineering of these mutations in *P. falciparum*. Mutations in these active site residues may lead to altered enzyme specificity, thereby excluding the antimetabolite from altering its activity. Notably, the generation of antimetabolites and interference with CoA-dependent processes in host cells is a potential source of unwanted side effects. However, we did not observe a high amount of antimetabolite formation in primary human hepatocytes, nor did we observe acute toxic effects or adverse events in rats or mice upon administration of oral doses up to 200 mg/kg, suggesting a specificity for the parasite enzymes over the host enzymes.

Although these new pantothenamides hold promise for future drug development, drug discovery is challenging, and thus experimental limitations need to be considered. Our combined genetic and metabolomics data suggest that the mechanism of action and the mechanism of resistance overlap for the pantothenamides presented here. Whereas we demonstrate that treatment of parasites with these compounds resulted in decreased acetyl-CoA, formal proof that the CoA antimetabolite inhibits CoA binding enzymes is currently lacking. Generation of the CoA antimetabolite through synthetic chemistry to enable enzyme inhibition assays has proven to be challenging and is the subject of our continuing studies. While our data show that pantothenamides are converted into a CoA analog and suppress acetyl-CoA formation in both asexual and sexual blood-stage parasites, we also observed parasite stage specificity related to subtle changes in the pantothenamide chemical structure or competition by excess pantothenate. The molecular mechanisms for these stage-specific effects are not well understood, and an alternative target for pantothenamides in sexual stages cannot be ruled out. Our in vivo data show that parasite clearance continues even when compound concentrations in plasma drop below the in vitro efficacious level. Although the nature of the continued killing effect is not fully understood, it may originate from compound or metabolites accumulating in parasites or red blood cells. Last, although the predicted pharmacokinetics in humans is favorable, this is based on studies in three animal species, and further allometry studies involving multiple species will be required. Further development of a pantothenamide clinical candidate and prediction of the efficacious human dose will require a better understanding of the exposure-effect relationship.

In conclusion, our study identifies stable pantothenamide bioisosteres as antimalarial compounds with a new mode of action. These compounds are equally active against the parasite stages that cause clinical disease and those that drive onward transmission via the mosquito vector. These pantothenamide compounds provide important starting points for the development of next-generation drugs that could be combined with existing antimalarial drugs to effectively treat malaria.

MATERIALS AND METHODS

Study design

The objective of this study was to explore the potential of pantothenamide analogs as antimalarial agents. Synthetic chemistry in combination with in vitro parasitological assays was used to understand structure-activity relationships and to generate potent bioisosteres that are resistant to pantetheine-mediated degradation. A subset of molecules was tested against the different life cycle stages of the human malaria parasite *P. falciparum* to assess the potential for blockade of disease transmission and prevention of liver stage infection. Metabolomic analyses of *P. falciparum* parasites and human red blood cells were conducted to investigate the metabolic fate of compounds and their effects on the CoA biosynthesis pathway. To understand the mechanism of resistance, in vitro evolution experiments were conducted and the role of individual mutations in the resistance phenotype was studied using genetically engineered parasites. Last, the in vivo efficacy and pharmacokinetics of the lead pantothenamide MMV689258 was studied in a humanized mouse model of *P. falciparum* infection.

Data inclusion was based on performance of positive and negative controls that were included in all assays. In cases where the controls strongly deviated from their historical values, experiments were considered as failed and excluded from the analyses. All experiments were performed multiple times, and the number of replicates is indicated in the figure legends.

Chemistry

Unless noted otherwise, materials were purchased from commercial suppliers and used as received. Synthesis, ^{1}H–nuclear magnetic resonance (NMR) and ^{13}C-NMR spectra, and high-resolution MS (HRMS) of compounds described and tested in the main text are provided in Supplementary Materials and Methods. Synthesis, ^{1}H-NMR, and HRMS data of additional compounds to illustrate structure-activity relationship (listed in table S1) are given in Supplementary Materials and Methods.

Serum stability of pantothenamides

The stability of pantothenamides was measured after incubation for 16 hours at room temperature in 500 μM phosphate buffer (pH 7.4) with or without 10% fetal bovine serum as a source of pantetheinase activity. Samples were taken and analyzed by LC-MS using a Shimadzu LC10ATVP HPLC coupled to a Shimadzu LCMS-2010A mass spectrometer.

In vitro parasite cultures and assays

P. falciparum strain NF54 was cultured in RPMI 1640 medium supplemented with 25 mM $NaHCO_3$, 10% human type A serum, and 5% (v/v) human type 0 red blood cells (Sanquin, the Netherlands) in a semiautomated culture system (*43*). Replication assays for asexual blood-stage parasites were performed using a modification of a previously described SYBR Green method (*44*). Briefly, parasites were diluted in RPMI 1640 medium with 10% human serum to a parasitemia of 0.83% and a hematocrit of 3%. Thirty microliters of diluted parasites was combined with 30 μl of compound serially diluted in dimethyl sulfoxide (DMSO) and RPMI 1640 medium to reach a final DMSO concentration of 0.1% in a total assay volume of 60 μl. After a 72-hour incubation at 37°C, 3% O_2, and 4% CO_2, 30 μl of diluted SYBR Green reagent was added according to the instructions of the manufacturer (Life Technologies), and fluorescence intensity was quantified using a BioTek Synergy 2 plate reader. Pantothenate competition assays were performed by combining compounds with different concentrations of calcium-D-pantothenate (Sigma-Aldrich). Activity against asexual blood-stage parasites from a panel of drug-resistant strains was determined using ^{3}H-hypoxanthine incorporation assays as described before (*45*). Gametocyte viability assays were initiated by inoculating a culture flask with 1% asexual blood-stage parasites in 5% hematocrit in RPMI 1640 medium with 10% human serum. From days 4 to 9 after inoculation, cultures were treated with 50 mM *N*-acetylglucosamine to eliminate asexual blood-stage parasites. At day 11, after inoculation, gametocytes (predominantly stage IV) were isolated by Percoll density gradient centrifugation as described previously (*46*). Gametocytes were seeded at a density of 5000 cells per well in a 384-well plate and combined with compound diluted in DMSO and subsequently in RPMI 1640 medium to reach a final DMSO concentration of 0.1% in a volume of 60 μl of RPMI 1640 medium with 10% human serum. After a 72-hour incubation at 37°C, 3% O_2, and 4% CO_2, 30 μl of ONE-Glo reagent (Promega) was added, and luminescence was quantified using a BioTek Synergy 2 reader. Effect of compounds on development of *P. falciparum* liver stages in human primary hepatocytes was analyzed essentially as

described before (*47*). Briefly, 50,000 human primary hepatocytes were seeded in collagen-coated 96 plates according to the supplier's protocol (tebu-bio) and combined with compounds serially diluted in DMSO and culture medium to achieve a final DMSO concentration of 0.1%. Hepatocytes were infected with 50,000 *P. falciparum* NF54 sporozoites per well, and developing liver schizonts were visualized 4 days after infection by a 4′,6-diamidino-2-phenylindole nuclear stain and α-Hsp70 immunostaining as described before (*47*).

For asexual metabolomics studies, all parasites were grown in standard RPMI 1640 containing ~1 μM pantothenic acid and supplemented with 0.25% AlbuMAX II (Gibco) unless otherwise noted. 3D7 was cultured and magnetically purified as previously described (*34*), and NF54 was used for all gametocyte metabolomics studies. Induction (day −2) of NF54 gametocytes for metabolomics was performed by the addition of 1 volume of minimal fatty acid RPMI 1640 (15 μM palmitic and oleic acid only) to a culture of ~10% late ring-stage parasites [22 to 26 hours post infection (hpi)]. This addition was performed without removing the spent media from ~24 hours of growth (1× spent media:1× minimal fatty acid media). On day −1, the culture was split to ~2% parasitemia with fresh media, when the parasites reach the early schizont stage (~38 hpi). On the following day (day +1), a smear was made, and media were replaced to ensure that healthy rings were present, a population of which are committed to gametocytogenesis. On day +2, media were replaced with 2× volumes of media containing heparin (20 U/ml) to kill off the replicating asexual parasites. Heparin media changes (1× volume) were performed on days +3 and +4. Normal media changes resumed on days +5 and +6 after confirmation of asexual removal. On day +7, stage III/IV NF54 gametocytes were purified for metabolomics using the same protocol listed above for 3D7 asexual parasites.

Pulse-chase replication assays

Uninfected red blood cells were preloaded with 100 μM compound (MMV689258, chloroquine, or dihydroartemisinin), incubated at 37°C, and washed thoroughly to wash out the compound. Late trophozoite to schizont stage parasites were magnetically purified and diluted in preloaded uninfected red blood cells to a parasitemia of 0.83%, 3% hematocrit in a total assay volume of 100 μl. After a 72-hour incubation at 37°C, 3% O_2, and 4% CO_2, 100 μl of diluted SYBR Green reagent was added according to the instructions of the manufacturer (Life Technologies), and fluorescence intensity was quantified using a Synergy HTX Multi-Mode Reader (BioTek). Metabolomics pulse-chase assays were performed by seeding uninfected red blood cells into a 15-ml flask at a density of 1×10^8 cells/ml in RPMI 1640 media (~1% hematocrit). Red blood cells were preincubated for 1 hour before treatment with 1 μM MMV689258 (<0.01% DMSO) or no drug for 3 hours. After 3 hours, triplicate 1-ml samples were collected from each condition for metabolite extraction (see extraction protocol below). The remaining culture was centrifuged, washed with 1× volume of RPMI, resuspended to the original red blood cell density, and seeded into a 12-well plate at 1×10^8 cells per well in 2.5 ml of RPMI media (~0.4% hematocrit). Additional triplicate extractions were performed for each condition at 24-hour intervals after washout and up to 72 hours after, without subsequent media changes.

Selection of drug-resistant parasites and fitness assays

P. falciparum strain NF54 was cultured in a semiautomated system as described above and exposed to 30 nM (three times the IC_{50}) CXP18.6-052 to select for drug-resistant parasites. After reappearance and stable growth of surviving parasites, cultures were exposed to 10 times the IC_{50} (90 nM) and subsequently to 50 times the IC_{50} (450 nM). After stable growth of surviving parasites, limited dilution was performed in 96-well plates to isolate single-cell clones. Drug sensitivity of the resulting clones was analyzed by parasite replication assays as described above. Fitness assays were performed according to Peters *et al.* (*48*). Briefly, NF54 and a mutant parasite were mixed at a ratio of 1:1 and subcultured biweekly for 4 weeks in the absence of drug pressure. Samples were taken at regular intervals, and the relative presence of wild-type and mutant *ACS* alleles was assessed by multiplex PCR using primers MWV511 and MWV519 to detect wild-type (T627) *ACS* and primers MWV512 and MWV516 to detect the mutant (627A) allele. Details of primers are provided in table S9. PCR conditions were optimized using a DNA standard comprising wild-type and mutant genomic DNA at preset ratios ranging from 30:1 to 1:30. PCR products were separated on a 1.5% agarose gel, and relative quantities were analyzed by densitometry using the FIJI software package. Signals were corrected for background, and relative intensities were expressed as a percentage of the total amount of amplified DNA.

CRISPR-Cas9 gene editing of *P. falciparum*

To validate the mutations identified in the drug-induced resistant parasites, we introduced the point mutations using the CRISPR-Cas9 system. Parasites were transfected by invasion of DNA-loaded red blood cells as described previously (*49*). Briefly, 60 to 100 μg of plasmid was loaded into red blood cells by electroporation (310 V, 950 μF). A synchronized trophozoite culture was added to the DNA-loaded cells. One day after transfection, parasites were treated with selection drug for 5 days and cultured until they recovered. Clones of all mutants were obtained by limiting dilution, and integration was confirmed by Sanger sequencing.

The *ACS*-T627A substitution was generated in NF54 parasites using the pUF1-Cas9 plasmid (*50*), which expressed Cas9, and the plasmid pDC2-based human dihydrofolate reductase (h*DHFR*) [a gift from M. Lee, (*51*)]. The guide RNA was inserted in this latter plasmid using the Bbs I restriction site. Subsequently, the donor template, containing the desired mutation and two shield mutations, was cloned using Nhe I/Not I restriction sites. Parasites were selected with 1.5 μM DSM1 (Merck) and, after recovery, selected with 8× IC_{50} of MMV689258 for 3 days. To obtain genetically engineered parasites harboring both *ACS* and *ACS11* mutations, either of the *ACS11* mutations was introduced in the *ACS*-T627A mutant using a similar pDC2-based plasmid that also expressed Cas9. As an alternative approach, the mutations were reverted in the drug-induced resistant parasites. The guide RNA and donor template were cloned using the Bbs I restriction site and Aat II/Bam HI restriction sites, respectively; both were verified by Sanger sequencing. Parasites were selected with 2.5 nM WR99210.

Specific primers were designed for each point mutation to insert the three mutations in a donor template. Donor DNA was amplified by overlap extension PCR amplification from genomic *P. falciparum* DNA. Guide RNAs were ordered as oligonucleotides (Sigma-Aldrich). Details of primers for generating the plasmids and sequencing are provided in table S9.

Hepatocyte culture and cytotoxicity assays

Human primary hepatocytes (XenoTech 098H1500.H15B+) were thawed and plated in a collagen-coated 96-well plate in Williams E

medium (Gibco 32551087) supplemented with 1% Pen Strep (Gibco 15140-122), 1% fungizone (Gibco 15290026), 10% heat-inactivated fetal bovine serum (Gibco 10270-106), insulin (0.1 IU/ml; Sigma-Aldrich I2643), and 7 μM hydrocortisone hemisuccinate (Sigma-Aldrich H2270) and refreshed daily. After 2 days of culture, compounds were added and incubated in a humidified incubator at 37°C and 5% CO_2 for 78 hours (refreshed daily), followed by an additional 18-hour incubation with 700 μM resazurin (Sigma-Aldrich 199303). Fluorescence was read at BioTek Synergy 2, and data were analyzed in GraphPad Prism version 5.03.

In vitro pharmacokinetics

Plasma protein binding and in vitro hepatocyte metabolism data were obtained through a commercial service using their standard protocols (TCG Lifesciences, Kolkata, India). CYP450 inhibition data and CaCo transport data were generated by the Center for Drug Candidate Optimisation at Monash University, Australia, using previously described methods (*52*).

In vivo pharmacokinetics

Blood pharmacokinetics in male BALB/c mice were studied by intravenous injection of 3 mg/kg compound formulated in 5% (v/v) DMSO and 0.9% (w/v) NaCl, and oral gavage of 30 mg/kg compound formulated in 5% (v/v) DMSO, 0.1% (v/v) Tween 80, and 0.5% (w/v) carboxymethylcellulose in water. Animals were fasted 4 hours before and 2 hours after dosing. At time points indicated in the figures, about 50 μl of blood was collected into heparinized capillary tubes by piercing the saphenous vein with a needle. Plasma was collected after centrifugation at 1640*g* for 5 min at +4°C within half an hour of collection. Plasma samples were stored at −20°C until bioanalysis. Quantitation of compound concentrations was provided by a commercial service (TCG Lifesciences, Kolkata, India) using their standard LC-MS protocols. Plasma pharmacokinetics in male Sprague-Dawley rats was studied using identical dosing and analyses schemes. Rats were fasted 12 hours before and 2 hours after dosing.

Biliary and renal clearance was assessed by intravenous dosing of 3 mg/kg compound formulated in 2% (v/v) DMSO and 0.9% (w/v) NaCl to male Han Wistar rats. Bile was collected from bile duct cannulated rats for 0 to 1, 1 to 3, 3 to 8, 8 to 24, and 24 to 48 hours after dosing. Urine was collected for 0 to 6, 6 to 24, and 24 to 48 hours after dosing from rats housed in metabolic cages. Bioanalyses were performed by a commercial supplier (XenoGesis Ltd.) using their standard protocols.

In vivo efficacy studies in humanized mice

Reduction of existing parasitemia in vivo was investigated using a humanized mouse model for *P. falciparum* infection. Female NODscidIL2Rγ^{null} mice were engrafted by daily intravenous injection of 0.6 ml of human blood for 11 days. Subsequently, mice were infected with *P. falciparum* strain Pf3D7$^{0087/N9}$ (*53*) by injecting 2×10^7 parasites in a volume of 0.2 ml. Four days after infection, SCID mice were treated with either vehicle control, MMV689258, or chloroquine. To this end, compounds were formulated in 70% Tween 80 ($d = 1.08$ g/ml) and 30% ethanol ($d = 0.81$ g/ml), followed by a 10-fold dilution in H_2O and administered by oral gavage. Parasitemia was followed by daily collection of 2 μl of tail blood. The hematocrit was determined by fluorescence-activated cell sorting and parasitemia was determined by microscopy on >10,000 red blood cells as described before (*53*). For pharmacokinetic analyses of samples from the SCID mice, peripheral blood samples (20 μl) were taken at different times as indicated in the figure legends, mixed with 20 μl of ultrapure H_2O, immediately frozen on dry ice, and stored at −80°C until analysis. Blood samples were processed under liquid-liquid extraction conditions and analyzed by LC-MS/MS for quantification using a commercial service using their standard protocols (Swiss BioQuant, Basel, Switzerland).

Compound effects on parasite transmission to the mosquito vector were assessed by luminescent standard membrane-feeding assays. To this end, mature stage V gametocytes of transgenic reporter strain NF54-HGL were incubated for 24 hours with compound before mosquito feeding as described before (*32*). Similarly, gametocytes from drug-resistant clone F49C11 were fed to *A. stephensi* mosquitoes to assess whether the mutations affect transmission to the mosquito vector.

Metabolomics analyses

Extraction and analysis were performed as previously demonstrated (*34*). Briefly, trophozoite stage 3D7 parasites were magnetically purified, allowed to recover in RPMI1640 (0.25% AlbuMAX II) at 0.4% parasitemia (1×10^8 cells/sample), and treated with drug (10× IC_{50}) for 2.5 hours. After treatment, parasites were pelleted, washed with 1 ml of ice-cold 1× phosphate-buffered saline (PBS), and extracted using 1 ml of ice-cold 9:1 MeOH/water, containing the internal standard $^{13}C_4$,$^{15}N_1$-aspartate. Supernatants were clarified before drying under nitrogen, followed by resuspension in HPLC grade water containing 1 μM chlorpropamide to 1×10^6 parasites/μl for HPLC-MS analysis. Ten microliters was injected on a Thermo Exactive Plus Orbitrap MS for HPLC-MS–based targeted metabolomics [modified from Lu *et al.* (*54*)]. The modifications were made to increase the separation and detection capabilities of late-eluting compounds and are as follows: gradients are 0 min = 0%B, 5 min = 20%B, 7.5 min = 55%B, 15 min = 65%B, 17.5 min = 95%B, and 21 min = 0%B; mass filters are 0 to 5 min, 85 to 800 mass/charge ratio (*m/z*); 5 to 6 min, 100 to 800 *m/z*; 6 to 9.5 min, 85 to 800 *m/z*; 9.5 to 15.5 min, 110 to 1000 *m/z*; and 15.5 to 22.5 min, 250 to 1000 *m/z* (the last 2.5 min are not scanned during reequilibration). All Orbitrap data were acquired using Phenomenex columns 00D-4387-B0 from batch 5380-0025. Data were processed using Maven as previously described from a targeted metabolite list (*34*) and using a ±10 parts per million *m/z* window and/or a 1-min retention time window from the data provided in table S2. Postprocessing was performed in Microsoft Excel using blank value imputation for compounds at/below background (i.e., avoiding values ≤0). Graphics were generated using a combination of Excel, R, and Adobe Illustrator. Metabolomics on NF54 drug-resistant clone F50D5 asexual blood-stage parasites was performed as described above. Gametocyte metabolomics was performed as above with a 1-μM treatment concentration; however, the seeding density was 5.5×10^7 parasites/sample with the same injection volume and concentration. Isotopically labeled standards were purchased from Cambridge Isotope Laboratories Inc. (Tewksbury, MA). Saponin lysis was performed as previously demonstrated (*8*) using magnetically purified parasites, and parasites were deemed viable through trypan blue staining and their ability to metabolize labeled pantothenic acid. Isolated parasites were washed with PBS and resuspended in pantothenate-free RPMI 1640 (0.25% AlbuMAX II; Gibco) to the same densities as above.

Recent inspection of cell banks has revealed potential contamination of the 3D7 strain with Dd2 parasites. It is possible that some

of the metabolomics experiments may have contained trace amounts of the Dd2 parasite line.

For analyses of the effects of compounds on CoA metabolism in human primary hepatocytes, cells were cultured in a 12-well plate as described above and 1.4×10^6 cells were incubated with 1 μM compound for 3.5 hours. Cells were then washed with ice-cold 1× PBS and extracted using 1 ml of ice-cold 70:30 MeOH/water, containing the internal standard $^{13}C_4$,$^{15}N_1$-aspartate. Additional processing was performed as with parasite samples, and the injection concentration was ~2.7×10^4 cells/μl. Primary hepatocytes were extracted in technical duplicate and pooled for a single LC-MS injection due to sample limitations.

Pantothenate quantification in serum

Levels of free pantothenate in human, mouse, and rat serum were quantified using the same LC-MS platform as used for the parasite metabolomics. The analytical method was modified to scan a narrower range (85 to 300 *m/z*) up until 15.5 min to improve the sensitivity and linear range. Briefly, a 100-μl serum sample was spiked with 1 μM ^{13}C3,^{15}N1-pantothenate, followed by extraction with 9 volumes of ice-cold MeOH. Samples were centrifuged, and supernatants were dried under nitrogen and resuspended in 100 μl of HPLC grade water containing 1 μM fully labeled 13C9,15N1-tyrosine (used for injection normalization). An external calibration curve, consisting of seven dilutions of unlabeled pantothenic acid (25 to 18.225 μM) spiked with 1 μM 13C3,15N1-pantothenate, was generated during the same analytical run as the samples. The peak intensities were used to plot the ratio of labeled pantothenate versus unlabeled pantothenate against the pantothenate concentration. The calibration curve displayed linearity with an R^2 value of 0.9998. The resulting relative response factor ratio was used to quantify the amount of pantothenate in the extracted serum samples. All samples were extracted in technical triplicate, and 20 μl of extract was injected per sample.

Whole genome sequencing

Genomic DNA was isolated from parasites using a DNeasy Blood & Tissue Kit according to the instructions of the manufacturer (Qiagen). Library preparation was performed as previously demonstrated (*55*). Briefly, Illumina barcoded DNA quality was assessed using an Agilent 2100 Bioanalyzer and Qubit before samples were sequenced using an Illumina HiSeq 2500 system (Penn State Genomics Core Facility). Sequencing outputs were uploaded into a local instance of Galaxy and quality was assessed by FastQ. Sequences were trimmed using trimmomatic, and mapping was performed using the 3D7 reference genome (www.plasmodb.org) and Next-Generation Sequencing Mapping (BWA-MEM) program. Files were filtered and converted to SAM/BAM for variant analysis by FreeBayes. Variants were identified and annotated using the SNPEff tool, followed by further selection using the SelectVariants and variant filtration tools. Visualization of the alignment and unique reads was performed using the Integrative Genomics Viewer. Mutations in the coding regions that were unique to the resistant line(s) but not the parental NF54 were denoted as important contributors. Read depth was manually assessed for genes of interest (pantothenate-CoA biosynthesis pathway) to ensure that there was no copy number variation between the tested parasite lines.

Generation of recombinant human PANKs

Recombinant human PANK1, PANK2, and PANK3 were cloned and expressed using a bacterial expression system. The gene encoding human PANK1β was mutagenized using the QuikChange site-directed mutagenesis kit (Stratagene) with primers that added a Nhe I restriction site to the NH2-terminus and a Xho I restriction site to the COOH-terminus. The PCR product was cloned into pET28a to obtain an NH_2-terminal His_6-tag fusion protein, and the resulting plasmid was transformed into the *E. coli* BL21(DE3) (Stratagene) expression strain. The cells were grown to mid-log phase, and the protein was induced with 1.0 mM isopropyl-β-D-thiogalactopyranoside for 18 hours at 16°C. The PANK1β protein was purified using a nickel–nitrilotriacetic acid affinity column and eluted with 50 mM tris (pH 7.9), 500 mM NaCl, 10% glycerol, and 300 mM imidazole. The purified protein was dialyzed overnight at 4°C in 20 mM tris (pH 7.5) and 300 mM NaCl and stored at −80°C in equal volume glycerol until further use. The genes encoding the mature form of human PANK2 (residues 141 to 570) and the catalytic core domain of human PANK3 (residues 12 to 368) were similarly cloned and purified as previously reported (*56*, *57*).

Generation of recombinant *Pf*PANK1

Recombinant *Pf* PANK1 used for immunization was obtained by cloning the cDNA corresponding to the open reading frame that encodes the full-length *Pf* PANK1 protein into the baculovirus transfer vector pFastBac HT in frame with an N-terminal six-histidine purification tag. *Pf* PANK1 protein was produced with the baculovirus expression system at the St. Jude Children's Research Hospital Protein Production Facility. Bacmid production, transfection, and baculovirus amplification were carried out according to the manual (Invitrogen). Suspension cultures of *Sf*9 cells were cultured in SFX-insect serum-free media to a density of 2×10^6 cells/ml and infected at a multiplicity of infection of 10. Cultures were gently shaken for 3 days at 28°C, harvested, and resuspended in a buffer containing 50 mM tris (pH 7.9), 500 mM NaCl, and 10% glycerol and lysed by microfluidization. Cell lysates were clarified by centrifugation at 20,000 rpm, and soluble *Pf*PANK1 was purified from the supernatant by HiTrap Ni^{2+}metal affinity chromatography and eluted with 50 mM tris (pH 7.9), 500 mM NaCl, 10% glycerol, and 1 M imidazole. Purified *Pf* PANK1 was dialyzed into 50 mM tris (pH 7.9), 500 mM NaCl, and 10% glycerol flash-frozen in liquid nitrogen and stored at −80°C until further use.

Generation of polyclonal antiserum and immunoprecipitation assays

Rabbits were immunized with recombinant *Pf* PANK1 according to standard procedures of the manufacturer (Eurogentec, Seraing, Belgium). Reactivity of serum was compared with preimmune serum using an enzyme-linked immunosorbent assay on plates coated with 50 ng of antigen per well. A dilution range of serum (preimmune serum and serum from the final bleed after immunization) was tested. Antibody binding was measured using the Vectastain ABC kit (Vector Laboratories) with a biotinylated goat anti-rabbit secondary antibody. Immunoglobulins were absorbed on protein A/G Sepharose (Pierce) and used to isolate *Pf* PANK1 from parasite lysates. PANK assay, as described below, was performed on the immunoprecipitated material and the depleted parasite lysates.

Parasite lysates for *Pf*PANK assay

Asynchronous blood-stage parasites from *P. falciparum* strain NF54 were released from the red blood cells by lysis with 0.06% saponin in PBS for 5 min on ice. Parasites were pelleted by centrifugation (10 min at 4000*g*), washed with PBS, and lysed in 50 mM NaF, 20 mM

tris-HCl (pH 7.5), 0.1% Triton X-100, 2 mM dithiothreitol, 2 mM EDTA, and 1% (v/v) Halt Protease Inhibitor Cocktail (ThermoFischer Scientific, Waltham, MA, USA). Suspensions were then sonicated six times for 3 s at an amplitude of 16 μm peak to peak. Sonicated samples were centrifuged at 15,000 rpm for 5 min at 4°C, and supernatants were used in immunoprecipitation and enzyme activity assays.

PANK assay

PANK activity was monitored using a radioactive labeled PANK assay. The reaction mixtures contained 10 mM $MgCl_2$, 2.5 mM adenosine triphosphate, 5 μM ^{14}C-labeled pantothenate, 100 mM tris-HCl (pH 7.4), the to-be-tested pantothenamide and enzyme (freshly prepared *P. falciparum* lysate), and recombinant protein in a total volume of 40 μl. Reactions were initiated after addition of enzyme and incubated at 37°C for 60 min. Reaction was terminated with 4 μl of a 10% acetic acid solution in 95% ethanol. Samples were loaded on diethylaminoethyl filter discs (GE Healthcare) and washed thoroughly in 1% acetic acid solution in 95% ethanol. Phosphorylated pantothenate will stay on the filter, whereas the unphosphorylated pantothenate will be washed away. After the discs were dried, they were transferred into scintillation vials containing 3 ml of ScintiSafe 30% cocktail (Fischer Scientific, Hampton, NH, USA). Radioactivity in each vial was counted using a Tri-Carb 2900TR Liquid Scintillation Analyzer (Packard BioScience, Boston, MA). Inhibition assays were performed in the presence of compound in a serial dilution range varying from 100 μM to 10 nM. IC_{50} values were calculated with GraphPad Prism version 5.03.

Statistics

IC_{50} values were determined by logistic regression using a four-parameter model and the least squares method to find the best fit. Analysis of variance (ANOVA) and Student's *t* tests were performed. The specific test applied is indicated in the respective figure legends. Individual-level data are provided in table S10.

SUPPLEMENTARY MATERIALS

stm.sciencemag.org/cgi/content/full/11/510/eaas9917/DC1
Materials and Methods
Fig. S1. Pantothenamide stability.
Fig. S2. Parasite life cycle.
Fig. S3. Pantothenate competition assays.
Fig. S4. PANK activity.
Fig. S5. Expression of *Pf*PANK1.
Fig. S6. Cellular pantothenamide metabolism and targeted metabolomics.
Fig. S7. Pantothenate and pantothenamide metabolism in saponin-isolated parasites versus uninfected red blood cells.
Fig. S8. Erythrocytes preexposed to MMV689258 are less susceptible to malaria infection.
Fig. S9. Drug-resistant parasite (*ACS*-T627A and *ACS*11-E660K) transmission to mosquitoes.
Fig. S10. Pantothenamide-resistant parasites (*ACS*-T627A and *ACS11*-E660K) have reduced fitness.
Fig. S11. Sequence verification of CRISPR-Cas9–engineered mutations.
Fig. S12. Metabolomics of wild-type versus drug-resistant parasites.
Fig. S13. Pharmacokinetics of MMV689258 in rodents.
Fig. S14. Dose-normalized plasma exposure of MMV689258 in NODscidIL2Rγ^{null} mice.
Fig. S15. Red blood cell counts in *Pf*SCID mice treated with MMV689258.
Fig. S16. Cell-type specificity and primary human hepatocyte metabolomics.
Table S1. Selection of compounds to illustrate structure-activity relationship.
Table S2. IC_{50} values of compounds shown in Fig. 1.
Table S3. Description of strains used in resistance panel.
Table S4. Targeted metabolomics values for select compounds of interest.
Table S5. Pharmacokinetic parameters derived from the data shown in fig. S13.
Table S6. Renal excretion of MMV689258 in rats.
Table S7. Biliary excretion of MMV689258 in rats.
Table S8. In vitro ADME parameters of MMV689258.
Table S9. Primers used for genetic studies.
Table S10. Source data for Figs. 1C, 2 (A to E), 3C, 4B, and 5 (A to C).

REFERENCES AND NOTES

1. WHO, "World Malaria Report 2016, ISBN: 978 92 4 151171 1," (2016).
2. L. H. Miller, H. C. Ackerman, X.-z. Su, T. E. Wellems, Malaria biology and disease pathogenesis: Insights for new treatments. *Nat. Med.* **19**, 156–167 (2013).
3. J. N. Burrows, S. Duparc, W. E. Gutteridge, R. Hooft van Huijsduijnen, W. Kaszubska, F. Macintyre, S. Mazzuri, J. J. Möhrle, T. N. C. Wells, New developments in anti-malarial target candidate and product profiles. *Malar. J.* **16**, 26 (2017).
4. A. A. Divo, T. G. Geary, N. L. Davis, J. B. Jensen, Nutritional requirements of *Plasmodium falciparumin* culture. I. Exogenously supplied dialyzable components necessary for continuous growth. *J. Protozool.* **32**, 59–64 (1985).
5. F. Y. Wiselogle, *A Survey of Antimalarial Drugs* (J. W. Edwards, 1946).
6. A. M. Lehane, R. V. Marchetti, C. Spry, D. A. van Schalkwyk, R. Teng, K. Kirk, K. J. Saliba, Feedback inhibition of pantothenate kinase regulates pantothenol uptake by the malaria parasite. *J. Biol. Chem.* **282**, 25395–25405 (2007).
7. K. J. Saliba, I. Ferru, K. Kirk, Provitamin B_5 (pantothenol) inhibits growth of the intraerythrocytic malaria parasite. *Antimicrob. Agents Chemother.* **49**, 632–637 (2005).
8. K. J. Saliba, H. A. Horner, K. Kirk, Transport and metabolism of the essential vitamin pantothenic acid in human erythrocytes infected with the malaria parasite *Plasmodium falciparum*. *J. Biol. Chem.* **273**, 10190–10195 (1998).
9. C. Spry, K. J. Saliba, The human malaria parasite *Plasmodium falciparum* is not dependent on host coenzyme A biosynthesis. *J. Biol. Chem.* **284**, 24904–24913 (2009).
10. C. Spry, K. Kirk, K. J. Saliba, Coenzyme A biosynthesis: An antimicrobial drug target. *FEMS Microbiol. Rev.* **32**, 56–106 (2008).
11. G. Clifton, S. R. Bryant, C. G. Skinner, N^1-(substituted) pantothenamides, antimetabolites of pantothenic acid. *Arch. Biochem. Biophys.* **137**, 523–528 (1970).
12. E. Strauss, T. P. Begley, The antibiotic activity of *N*-pentylpantothenamide results from its conversion to ethyldethia-coenzyme A, a coenzyme A antimetabolite. *J. Biol. Chem.* **277**, 48205–48209 (2002).
13. Y.-M. Zhang, M. W. Frank, K. G. Virga, R. E. Lee, C. O. Rock, S. Jackowski, Acyl carrier protein is a cellular target for the antibacterial action of the pantothenamide class of pantothenate antimetabolites. *J. Biol. Chem.* **279**, 50969–50975 (2004).
14. R. Leonardi, S. Chohnan, Y.-M. Zhang, K. G. Virga, R. E. Lee, C. O. Rock, S. Jackowski, A pantothenate kinase from *Staphylococcus aureus* refractory to feedback regulation by coenzyme A. *J. Biol. Chem.* **280**, 3314–3322 (2005).
15. P. L. J. M. Zeeuwen, P. A. M. Jansen, J. Schalkwijk, F. P. J. T. Rutjes, B. Ritzen, P. H. H. Hermkens, Pantothenic acid derivatives and their use in the treatment of microbial infections, Patent application WO2011152720 (2011).
16. C. Spry, C. Macuamule, Z. Lin, K. G. Virga, R. E. Lee, E. Strauss, K. J. Saliba, Pantothenamides are potent, on-target inhibitors of *Plasmodium falciparum* growth when serum pantetheinase is inactivated. *PLOS ONE* **8**, e54974 (2013).
17. P. A. M. Jansen, P. H. H. Hermkens, P. L. J. M. Zeeuwen, P. N. M. Botman, R. H. Blaauw, P. Burghout, P. M. van Galen, J. W. Mouton, F. P. J. T. Rutjes, J. Schalkwijk, Combination of pantothenamides with vanin inhibitors as a novel antibiotic strategy against gram-positive bacteria. *Antimicrob. Agents Chemother.* **57**, 4794–4800 (2013).
18. P. A. M. Jansen, J. A. van Diepen, B. Ritzen, P. L. J. M. Zeeuwen, I. Cacciatore, C. Cornacchia, I. M. J. J. van Vlijmen-Willems, E. de Heuvel, P. N. M. Botman, R. H. Blaauw, P. H. H. Hermkens, F. P. J. T. Rutjes, J. Schalkwijk, Discovery of small molecule vanin inhibitors: New tools to study metabolism and disease. *ACS Chem. Biol.* **8**, 530–534 (2013).
19. M. de Villiers, C. Macuamule, C. Spry, Y.-M. Hyun, E. Strauss, K. J. Saliba, Structural modification of pantothenamides counteracts degradation by pantetheinase and improves antiplasmodial activity. *ACS Med. Chem. Lett.* **4**, 784–789 (2013).
20. C. J. Macuamule, E. T. Tjhin, C. E. Jana, L. Barnard, L. Koekemoer, M. de Villiers, K. J. Saliba, E. Strauss, A pantetheinase-resistant pantothenamide with potent, on-target, and selective antiplasmodial activity. *Antimicrob. Agents Chemother.* **59**, 3666–3668 (2015).
21. J. E. Chiu, J. Thekkiniath, J.-Y. Choi, B. A. Perrin, L. Lawres, M. Plummer, A. Z. Virji, A. Abraham, J. Y. Toh, M. Van Zandt, A. S. I. Aly, D. R. Voelker, C. B. Mamoun, The antimalarial activity of the pantothenamide α-PanAm is via inhibition of pantothenate phosphorylation. *Sci. Rep.* **7**, 14234 (2017).
22. J. Schalkwijk, P. A. M. Jansen, P. H. H. Hermkens, P. N. M. Botman, Pantothenamide analogues, Patent application WO2016072854 (2016).
23. V. M. Howieson, E. Tran, A. Hoegl, H. L. Fam, J. Fu, K. Sivonen, X. X. Li, K. Auclair, K. J. Saliba, Triazole substitution of a labile amide bond stabilizes pantothenamides and improves their antiplasmodial potency. *Antimicrob. Agents Chemother.* **60**, 7146–7152 (2016).
24. M. de Villiers, C. Spry, C. J. Macuamule, L. Barnard, G. Wells, K. J. Saliba, E. Strauss, Antiplasmodial mode of action of pantothenamides: Pantothenate kinase serves as a metabolic activator not as a target. *ACS Infect. Dis.* **3**, 527–541 (2017).

25. E. T. Tjhin, C. Spry, A. L. Sewell, A. Hoegl, L. Barnard, A. E. Sexton, G. Siddiqui, V. M. Howieson, A. G. Maier, D. J. Creek, E. Strauss, R. Marquez, K. Auclair, K. J. Saliba, Mutations in the pantothenate kinase of *Plasmodium falciparum* confer diverse sensitivity profiles to antiplasmodial pantothenate analogues. *PLOS Pathog.* **14**, e1006918 (2018).
26. S. Kenthirapalan, A. P. Waters, K. Matuschewski, T. W. A. Kooij, Functional profiles of orphan membrane transporters in the life cycle of the malaria parasite. *Nat. Commun.* **7**, 10519 (2016).
27. R. J. Hart, L. Lawres, E. Fritzen, C. Ben Mamoun, A. S. I. Aly, *Plasmodium yoelii* vitamin B_5 pantothenate transporter candidate is essential for parasite transmission to the mosquito. *Sci. Rep.* **4**, 5665 (2014).
28. R. J. Hart, A. Abraham, A. S. I. Aly, Genetic characterization of coenzyme A biosynthesis reveals essential distinctive functions during malaria parasite development in blood and mosquito. *Front. Cell. Infect. Microbiol.* **7**, 260 (2017).
29. H. E. Pett, P. A. M. Jansen, P. H. H. Hermkens, P. N. M. Botman, C. A. Beuckens-Schortinghuis, R. H. Blaauw, W. Graumans, M. van de Vegte-Bolmer, K. M. J. Koolen, F. P. J. T. Rutjes, K. J. Dechering, R. W. Sauerwein, J. Schalkwijk, Novel pantothenate derivatives for anti-malarial chemotherapy. *Malar. J.* **14**, 169 (2015).
30. A. Hoegl, H. Darabi, E. Tran, E. Awuah, E. S. C. Kerdo, E. Habib, K. J. Saliba, K. Auclair, Stereochemical modification of geminal dialkyl substituents on pantothenamides alters antimicrobial activity. *Bioorg. Med. Chem. Lett.* **24**, 3274–3277 (2014).
31. J. Guan, M. Hachey, L. Puri, V. Howieson, K. J. Saliba, K. Auclair, A cross-metathesis approach to novel pantothenamide derivatives. *Beilstein J. Org. Chem.* **12**, 963–968 (2016).
32. M. W. Vos, W. J. R. Stone, K. M. Koolen, G.-J. van Gemert, B. van Schaijk, D. Leroy, R. W. Sauerwein, T. Bousema, K. J. Dechering, A semi-automated luminescence based standard membrane feeding assay identifies novel small molecules that inhibit transmission of malaria parasites by mosquitoes. *Sci. Rep.* **5**, 18704 (2015).
33. S. Jackowski, C. O. Rock, Regulation of coenzyme A biosynthesis. *J. Bacteriol.* **148**, 926–932 (1981).
34. E. L. Allman, H. J. Painter, J. Samra, M. Carrasquilla, M. Llinás, Metabolomic profiling of the malaria box reveals antimalarial target pathways. *Antimicrob. Agents Chemother.* **60**, 6635–6649 (2016).
35. A. D'Alessandro, P. G. Righetti, L. Zolla, The red blood cell proteome and interactome: An update. *J. Proteome Res.* **9**, 144–163 (2010).
36. J. Ducharme, R. Farinotti, Clinical pharmacokinetics and metabolism of Chloroquine. *Clin. Pharmacokinet.* **31**, 257–274 (1996).
37. S. Fletcher, L. Lucantoni, M. L. Sykes, A. J. Jones, J. P. Holleran, K. J. Saliba, V. M. Avery, Biological characterization of chemically diverse compounds targeting the *Plasmodium falciparum* coenzyme A synthesis pathway. *Parasit. Vectors* **9**, 589 (2016).
38. L. L. Bethke, M. Zilversmit, K. Nielsen, J. Daily, S. K. Volkman, D. Ndiaye, E. R. Lozovsky, D. L. Hartl, D. F. Wirth, Duplication, gene conversion, and genetic diversity in the species-specific acyl-CoA synthetase gene family of *Plasmodium falciparum*. *Mol. Biochem. Parasitol.* **150**, 10–24 (2006).
39. S. E. R. Bopp, M. J. Manary, A. T. Bright, G. L. Johnston, N. V. Dharia, F. L. Luna, S. McCormack, D. Plouffe, C. W. McNamara, J. R. Walker, D. A. Fidock, E. L. Denchi, E. A. Winzeler, Mitotic evolution of *Plasmodium falciparum* shows a stable core genome but recombination in antigen families. *PLOS Genet.* **9**, e1003293 (2013).
40. S. A. Cobbold, A. M. Vaughan, I. A. Lewis, H. J. Painter, N. Camargo, D. H. Perlman, M. Fishbaugher, J. Healer, A. F. Cowman, S. H. I. Kappe, M. Llinás, Kinetic flux profiling elucidates two independent acetyl-CoA biosynthetic pathways in *Plasmodium falciparum*. *J. Biol. Chem.* **288**, 36338–36350 (2013).
41. N. J. White, Pharmacokinetic and pharmacodynamic considerations in antimalarial dose optimization. *Antimicrob. Agents Chemother.* **57**, 5792–5807 (2013).
42. G. G. Zhanel, D. J. Hoban, G. K. M. Harding, The postantibiotic effect: A review of in vitro and in vivo data. *DICP* **25**, 153–163 (1991).
43. T. Ponnudurai, A. H. W. Lensen, J. F. G. M. Meis, J. H. E. T. Meuwissen, Synchronization of *Plasmodium falciparum* gametocytes using an automated suspension culture system. *Parasitology* **93**, 263–274 (1986).
44. V. Dery, N. O. Duah, R. Ayanful-Torgby, S. A. Matrevi, F. Anto, N. B. Quashie, An improved SYBR Green-1-based fluorescence method for the routine monitoring of *Plasmodium falciparum* resistance to anti-malarial drugs. *Malar. J.* **14**, 481 (2015).
45. C. Snyder, J. Chollet, J. Santo-Tomas, C. Scheurer, S. Wittlin, In vitro and in vivo interaction of synthetic peroxide RBx11160 (OZ277) with piperaquine in *Plasmodium* models. *Exp. Parasitol.* **115**, 296–300 (2007).
46. J. M. Bolscher, K. M. J. Koolen, G. J. van Gemert, M. G. van de Vegte-Bolmer, T. Bousema, D. Leroy, R. W. Sauerwein, K. J. Dechering, A combination of new screening assays for prioritization of transmission-blocking antimalarials reveals distinct dynamics of marketed and experimental drugs. *J. Antimicrob. Chemother.* **70**, 1357–1366 (2015).
47. A. Boes, H. Spiegel, R. Kastilan, S. Bethke, N. Voepel, I. Chudobová, J. M. Bolscher, K. J. Dechering, R. Fendel, J. F. Buyel, A. Reimann, S. Schillberg, R. Fischer, Analysis of the dose-dependent stage-specific in vitro efficacy of a multi-stage malaria vaccine candidate cocktail. *Malar. J.* **15**, 279 (2016).
48. J. M. Peters, N. Chen, M. Gatton, M. Korsinczky, E. V. Fowler, S. Manzetti, A. Saul, Q. Cheng, Mutations in cytochrome *b* resulting in atovaquone resistance are associated with loss of fitness in *Plasmodium falciparum*. *Antimicrob. Agents Chemother.* **46**, 2435–2441 (2002).
49. K. W. Deitsch, C. Driskill, T. E. Wellems, Transformation of malaria parasites by the spontaneous uptake and expression of DNA from human erythrocytes. *Nucleic Acids Res.* **29**, 850–853 (2001).
50. M. Ghorbal, M. Gorman, C. R. Macpherson, R. M. Martins, A. Scherf, J.-J. Lopez-Rubio, Genome editing in the human malaria parasite *Plasmodium falciparum* using the CRISPR-Cas9 system. *Nat. Biotechnol.* **32**, 819–821 (2014).
51. M. Y.-X. Lim, G. LaMonte, M. C. S. Lee, C. Reimer, B. H. Tan, V. Corey, B. F. Tjahjadi, A. Chua, M. Nachon, R. Wintjens, P. Gedeck, B. Malleret, L. Renia, G. M. C. Bonamy, P. C.-L. Ho, B. K. S. Yeung, E. D. Chow, L. Lim, D. A. Fidock, T. T. Diagana, E. A. Winzeler, P. Bifani, UDP-galactose and acetyl-CoA transporters as *Plasmodium* multidrug resistance genes. *Nat. Microbiol.* **1**, 16166 (2016).
52. M. A. Phillips, J. Lotharius, K. Marsh, J. White, A. Dayan, K. L. White, J. W. Njoroge, F. el Mazouni, Y. Lao, S. Kokkonda, D. R. Tomchick, X. Deng, T. Laird, S. N. Bhatia, S. March, C. L. Ng, D. A. Fidock, S. Wittlin, M. Lafuente-Monasterio, F. J. G. Benito, L. M. S. Alonso, M. S. Martinez, M. B. Jimenez-Diaz, S. F. Bazaga, I. Angulo-Barturen, J. N. Haselden, J. Louttit, Y. Cui, A. Sridhar, A. M. Zeeman, C. Kocken, R. Sauerwein, K. Dechering, V. M. Avery, S. Duffy, M. Delves, R. Sinden, A. Ruecker, K. S. Wickham, R. Rochford, J. Gahagen, L. Iyer, E. Riccio, J. Mirsalis, I. Bathhurst, T. Rueckle, X. Ding, B. Campo, D. Leroy, M. J. Rogers, P. K. Rathod, J. N. Burrows, S. A. Charman, A long-duration dihydroorotate dehydrogenase inhibitor (DSM265) for prevention and treatment of malaria. *Sci. Transl. Med.* **7**, 296ra111 (2015).
53. M. B. Jimenez-Diaz, T. Mulet, S. Viera, V. Gómez, H. Garuti, J. Ibañez, A. Alvarez-Doval, L. D. Shultz, A. Martínez, D. Gargallo-Viola, I. Angulo-Barturen, Improved murine model of malaria using *Plasmodium falciparum* competent strains and non-myelodepleted NOD-*scid IL2R*γ^{null} mice engrafted with human erythrocytes. *Antimicrob. Agents Chemother.* **53**, 4533–4536 (2009).
54. W. Lu, M. F. Clasquin, E. Melamud, D. Amador-Noguez, A. A. Caudy, J. D. Rabinowitz, Metabolomic analysis via reversed-phase ion-pairing liquid chromatography coupled to a stand alone orbitrap mass spectrometer. *Anal. Chem.* **82**, 3212–3221 (2010).
55. S. Pulcini, H. M. Staines, A. H. Lee, S. H. Shafik, G. Bouyer, C. M. Moore, D. A. Daley, M. J. Hoke, L. M. Altenhofen, H. J. Painter, J. Mu, D. J. P. Ferguson, M. Llinás, R. E. Martin, D. A. Fidock, R. A. Cooper, S. Krishna, Mutations in the *Plasmodium falciparum* chloroquine resistance transporter, PfCRT, enlarge the parasite's food vacuole and alter drug sensitivities. *Sci. Rep.* **5**, 14552 (2015).
56. B. S. Hong, G. Senisterra, W. M. Rabeh, M. Vedadi, R. Leonardi, Y.-M. Zhang, C. O. Rock, S. Jackowski, H.-W. Park, Crystal structures of human pantothenate kinases. *J. Biol. Chem.* **282**, 27984–27993 (2007).
57. R. Leonardi, Y.-M. Zhang, A. Lykidis, C. O. Rock, S. Jackowski, Localization and regulation of mouse pantothenate kinase 2. *FEBS Lett.* **581**, 4639–4644 (2007).

Acknowledgments: We thank J. Burrows for advice and discussion and the Lygature product development partnership for help with project management. A cDNA encoding *Pf*PANK1 was provided to S.J. by C. Ben Mamoun. M. Lee is acknowledged for contributing a pDC2-based gene targeting vector. We also thank the Huck Institutes of Life Sciences core facilities, Genomics Core Facility, and Metabolomics Core Facility at Penn State University. A. Patterson and P. Smith from the Penn State Metabolomics Core are acknowledged for technical and metabolomics expertise. We thank S. Charman and K. White from the Center for Drug Candidate Optimisation of Monash University for in vitro DMPK assays. We thank T. Mal, director of the Penn State University NMR facility, for assistance using the Bruker AVIII-HD-500 NMR and for help with spectral annotations. **Funding:** This work was supported by National Institutes of Health grant no. GM062896 (S.J.), Cancer Center Support grant no. CA21765 (S.J.), Medicines for Malaria Venture grant no. RD/14/0019 (K.J.D., M.L., and J.S.), Burroughs Wellcome Fund Investigators in Pathogenesis of Infectious Disease (PATH) Award (M.L.), NIH Ruth Kirschstein National Research Service Award (NRSA) Individual Postdoctoral Fellowship (F32) AI124507 (E.L.A.), and the American Lebanese Syrian Associated Charities (S.J.). T.W.A.K. was supported by the Netherlands Organization for Scientific Research (no. NWO-VIDI 864.13.009). The Illumina HiSeq 2500 (Penn State University) was purchased with NSF-MRI award no. DBI-1229046. The AB Sciex TripleTOF 5600 was purchased with NSF-MRI award no. CBET-1126373. **Author contributions:** J.S., P.H.H.H., and K.J.D. conceived the work and did overall supervision and analysis of parasitology, medicinal chemistry, biochemistry, and molecular biology. E.L.A. performed and analyzed metabolomics and whole genome sequencing data. P.A.M.J. performed and analyzed molecular biology and biochemistry assays. L.E.d.V., J.M.J.V., G.J., and M.W.V. performed molecular biology and generation of parasite mutants. M.L. designed, supervised, and analyzed metabolomics and whole genome sequencing data. S.J., K.M., and S.A.R. generated recombinant enzymes. P.N.M.B. and C.A.B.-S. performed organic chemistry experiments. H.P., K.M.J.K., J.M.B., and M.W.V. performed in vitro parasitology assays. T.W.A.K. and R.W.S. supervised parasite mutant generation and in vitro parasitology experiments. R.H.B. and F.P.T.J.R. supervised organic chemistry experiments.

G.T. designed and analyzed DMPK experiments. S.W., C.S., S.S., C.F., M.B.J.-D., and I.A.-B. performed efficacy and pharmacokinetics studies in SCID mice. B.C. advised on parasitology and drug development. J.S., E.L.A., P.A.M.J., L.E.d.V., M.L., and K.J.D. wrote the manuscript. All authors proofread and edited the manuscript. **Competing interests:** K.J.D. and R.W.S. hold stock in TropIQ Health Sciences B.V. Part of this work is described in patent application no. PCT/NL2015/050774, entitled "Pantothenamide Analogues" (coinventors P.H.H.H., P.A.M.J., J.S., and P.N.M.B.). E.L.A. is currently employed by Janssen Pharmaceuticals Inc. P.N.M.B. is currently employed by Aspen Healthcare. F.P.J.T.R. is a consultant of Enzyme Inc. and FutureChemistry Inc. S.J. is a member of the advisory board of CoA Therapeutics Inc. R.B. is a consultant for MMV and Potter Clarkson Inc. P.H.H.H. is a consultant for TropIQ Health Sciences B.V. **Data and materials availability:** All data associated with this study are present in the paper and/or the Supplementary Materials. Raw NMR spectra and metabolomics data have been deposited in the NIH metabolomics workbench repository. The project ID is PR000829, studies ST001239 and ST001238. Whole genome sequencing data (FastQ) of the lab-generated resistant parasite lines has been deposited in the NIH Sequence Read Archive (SRA) BioProject ID no. PRJNA560380. The genetically engineered *P. falciparum* parasite lines described here are available from T.W.A.K. under a material transfer agreement (MTA) with the Radboud University Medical Center. The pantothenamide compounds can be made available to researchers through an MTA by submitting a request to K.J.D.

Submitted 12 January 2018
Resubmitted 7 September 2018
Accepted 28 March 2019
Published 18 September 2019
10.1126/scitranslmed.aas9917

Citation: J. Schalkwijk, E. L. Allman, P. A. M. Jansen, L. E. de Vries, J. M. J. Verhoef, S. Jackowski, P. N. M. Botman, C. A. Beuckens-Schortinghuis, K. M. J. Koolen, J. M. Bolscher, M. W. Vos, K. Miller, S. A. Reeves, H. Pett, G. Trevitt, S. Wittlin, C. Scheurer, S. Sax, C. Fischli, I. Angulo-Barturen, M. B. Jiménez-Diaz, G. Josling, T. W. A. Kooij, R. Bonnert, B. Campo, R. H. Blaauw, F. P. J. T. Rutjes, R. W. Sauerwein, M. Llinás, P. H. H. Hermkens, K. J. Dechering, Antimalarial pantothenamide metabolites target acetyl–coenzyme A biosynthesis in *Plasmodium falciparum*. *Sci. Transl. Med.* **11**, eaas9917 (2019).

Abstract

One-sentence summary: Pantothenamides form antimetabolites that interfere with acetyl-CoA metabolism in the human malaria parasite *Plasmodium falciparum*.

Editor's Summary:
Development of a new antimalarial drug

Pantothenenic acid, or vitamin B5, is an essential nutrient for the deadly malaria parasite *Plasmodium falciparum*. Inhibiting the parasite's ability to fully metabolize this vitamin using pantothenamide drugs has long been considered a viable antimalarial therapeutic option. Historically, however, pantothenamides have not found success because of an enzyme in human serum that inactivates these molecules. In a new study, Schalkwijk *et al.* synthesize a series of pantothenamides that contained a modification of the labile bond, rendering them resistant to the action of this enzyme. The authors show that this new class of pantothenamides is converted by the parasite into coenzyme A analogs that are highly potent against malaria parasites at multiple stages of the *Plasmodium* life cycle.